Designing Response Supply Chain Against Bioattacks

David Simchi-Levi
Department of Civil and Environmental Engineering, Institute for Data, Systems, and Society, and the Operations Research Center, Massachusetts Institute of Technology, Cambridge, Massachusetts 02139, dslevi@mit.edu

Nikolaos Trichakis
MIT Sloan School of Management and Operations Research Center, Massachusetts Institute of Technology, Cambridge, Massachusetts 02139, ntrichakis@mit.edu

Peter Yun Zhang
Institute for Data, Systems, and Society, Massachusetts Institute of Technology, Cambridge, Massachusetts 02139, pyzhang@mit.edu

Bioattacks, *i.e.*, the intentional release of pathogens or biotoxins against humans to cause serious illness and death, pose a significant threat to public health and safety due to the availability of pathogens worldwide, scale of impact, and short treatment time window. In this paper, we focus on the problem of prepositioning inventory of medical countermeasures (MCM) to defend against such bioattacks. We introduce a two-stage robust optimization model that considers the policymaker's static inventory decision, attacker's move, and policymaker's adjustable shipment decision, so as to minimize inventory and life loss costs, subject to population survivability targets. We consider a heuristic solution approach that limits the adjustable decisions to be affine, which allows us to cast the problem as a tractable linear optimization problem. We prove that, under mild assumptions, the heuristic is in fact optimal. Experimental evidence suggests that the heuristic's performance remains near-optimal for general settings as well. We illustrate how our model can serve as a decision support tool for policy making. In particular, we perform a thorough case study on how to preposition MCM inventory in the United States to guard against anthrax attacks. We calibrate our model using data from multiple sources, including publications of the National Academies of Sciences and the U.S. Census. We find that, for example, if U.S. policymakers want to ensure a 95% survivability target for anthrax attacks that simultaneously affect at most two cities (in the same or different states), the minimum annual inventory budget required is approximately $330 million. We also discuss how our model can be applied in other contexts as well, *e.g.*, to analyze safety-stock placement in supply-chain networks to hedge against disruptions.

Key words: bioterrorism; supply chain design; robust optimization

1. Introduction

In this paper, we study the problem of prepositioning inventory of medical countermeasures (MCM) in preparation for bioattacks, *i.e.*, the intentional release of pathogens or biotoxins against humans to cause serious illness and death. Bioattacks have been a rising first-order concern to many coun-

tries worldwide in the last 15 years; the U.S. alone, for instance, has poured approximately $60 billion into biodefense preparedness since the 9/11 attacks [24]. Bioattacks are considered a major threat because a minute quantity of pathogens is sufficient to infect humans; furthermore, the corresponding MCMs need to be administered within a short time window to effectively reduce casualty. For example, if bioterrorists were to release *Bacillus anthracis*, *i.e.*, anthrax, over a large city, hundreds of thousands of people could be at risk, and MCMs would need to be administered to them within one to two days after the incubation period to have the intended effect [34, 43]. Distributing such large MCM quantities to the general public within such short time periods poses a considerable operational challenge, which is often compounded by attack detection delays.

In order to be prepared to deliver adequate medication in a timely manner in response to a bioattack, large amounts of MCMs need to be stockpiled at appropriate locations. Some inventories can be stored in central locations to take advantage of deployment flexibility, pooling effects, and scale economies in holding costs, while others can be positioned closer to populous areas, or even predispensed to the intended users in the form of home medical kits, in order to reduce transportation time should an adversarial event happen. Given a supply chain network of candidate storage locations, where and how much MCM inventory should then be prepositioned in order to cost-effectively defend against bioattacks? Our goal in this paper is to address this research question and develop a decision support framework that could guide policy design.

In the U.S., the Centers for Disease Control and Prevention (CDC) maintains MCM inventories within the Strategic National Stockpile (SNS),[1] which is a critical component of the national health security programs managed by the CDC's Office of Public Health Preparedness and Response (PHPR) [37, 36]. PHPR receives about $1.4 billion annually from Congress to strengthen the health security of the country, and three-quarters of the funding are allocated to SNS and the Public Health Emergency Preparedness (PHEP) cooperative agreements. While SNS holds MCMs under the command of federal authorities, PHEP provides guidelines and financial support to state and local public health departments to build more resilient communities in preparation for adverse health incidents. Therefore, the inventory storage and delivery mechanism of SNS, together with the preparedness infrastructure of PHEP, form a crucial line of defense for the nation's public health security.

For many bioattack threats, SNS stores MCM inventory centrally in order to leverage scale economies and keep costs low, while maintaining deployment flexibility. In particular, the logistics

[1] Apart from MCMs for bioattacks, the SNS includes a wide collection of medicines and medical supplies that provide disaster relief assets to the public during national emergencies, such as flu outbreaks, terrorist attacks, and natural disasters. Since its inception in the late 1990s, SNS has been deployed numerous times in a range of situations, including a 2001 anthrax attack, 9/11, hurricane Katrina, and the 2009 influenza pandemic. During the 2009 pandemic, for example, SNS successfully delivered 25% of the 44 million regimens of antiviral drugs to all 50 states.

and transportation infrastructure of the SNS central repositories is designed in a way that allows it to deploy any amount of stored MCMs to almost any major city in the U.S. within 12 to 36 hours, at negligible shipping costs.

But centrally stored inventories may not be responsive enough for events such as anthrax attacks. In recent years, public health officials have been increasingly aware of alternatives to centrally storing and managing SNS, namely the forward-deployment and prepositioning of MCMs to locations closer to the intended users. This problem has been raised as a first-order issue for the design and management of SNS and PHPR policymakers have commissioned several studies to examine different prepositiong strategies, for example, see [43]. To date, several key aspects of the problem have been identified and analyzed: location and transportation options for inventory prepositioning, financial cost of each system component, effects of time delay on health, and important design inputs such as the target protection level and time between attack and detection. However, a comprehensive cost-benefit analysis at the *system level* that *integrates* all these individual considerations into a practical quantitative decision support tool has been elusive. This gap is indeed highlighted in the following excerpt from a report [22] prepared by the Board of Scientific Counselors [35] for PHPR:

> "Both analytic and simulation (experimental) modeling activities should be increased substantially. Modeling will allow [the Division of] SNS to make quantitatively-based decisions on how much inventory to hold and where to hold it. An end-to-end model capturing the flow of materials in the SNS, as well as costs and logistical and health measures, should begin at the SNS-managed inventory site and go all the way to the point of dispensing to the public. Using such models will reveal bottlenecks, provide cost estimates, and help SNS properly evaluate the costs and consequences of alternative Response Supply Chain configurations."

The absence of an integrated model for MCM inventory prepositioning, both in practice and in the academic literature, attests to the underlying technical challenges, which stem primarily from the multiplicity of decisions facing policymakers—both strategic and operational—and the subtle way prepositioning could influence bioattackers' actions. In particular, on the strategic level, policymakers need to decide how much inventory to store among thousands of possible locations in anticipation of an attack. On the operational level, in the event a specific attack takes place, appropriate shipment decisions need to be made to efficiently dispense MCMs in a way that reflects the specific demand and supply conditions. Therefore, the *static* inventory positioning decisions need to be made in conjunction with myriads of *contingent* shipment policies. Furthermore, although some information about planned responses is already available in the public domain, prepositioning MCMs, particularly predispensing medical kits, is likely to grant to bioattackers even greater visibility to planned responses. Consequently, bioattackers, because they usually act in a pre-planned way

to inflict the greatest damage possible, are more likely to target under-served populated areas, as opposed to ones that have access to abundant stockpiles. This subtle interaction between defender and attacker's actions makes the demand for MCMs *endogenous* and challenging to model.

Our contributions

We propose a robust optimization (RO) model for the MCM prepositioning problem that addresses the aforementioned challenges. We model the SNS response supply chain as a network: inventory stockpiles as nodes, and shipment routes as links. Bioattacks correspond to demand surges at some of the network nodes. In that context, we cast the inventory prepositioning problem as a two-stage RO problem, with inventory placement decisions being first-stage (static) decisions and shipment decisions being second-stage (adjustable) decisions, contingent on the realized demand surge. The mini-max approach of RO allows us to capture the interaction between defender and attacker's actions we alluded to above. We calibrate the problem's objective and uncertainty set of possible demand scenarios in ways that reflect policymakers' considerations. In particular, we deal with minimizing either inventory holding costs under coverage guarantees under all possible attack scenarios, or worst-case holding and life loss costs, where possible scenarios comprise simultaneous attacks in multiple locations.

Multistage RO problems, however, are generally intractable, because the search for policies for the adjustable decisions makes the solution space infinite-dimensional. Therefore, we solve our problem via its so-called affinely adjustable robust counterpart [6], which reduces to a linear optimization problem by restricting the adjustable shipment policies to be affine in the demand shocks.

We make the following contributions.

1. *Modeling*: We provide an integrated framework for the MCM inventory prepositioning problem in a supply chain network that admits a tractable and scalable heuristic solution approach. Our model allows for a systematic tradeoff analysis of upstream versus downstream inventory placement, accounting for factors including deployment flexibility, pooling, holding costs, and responsiveness.
2. *Theory*: We prove that the affine adjustable policy heuristic is in fact optimal under mild and practical assumptions. We discuss the implications of our result for the RO literature at length in our literature review and in Section 4. Numerical studies we conducted confirmed that affine policies provide near-optimal performance for the inventory prepositioning problem under general settings as well.
3. *Designing SNS*: We perform a thorough case study of MCM inventory prepositioning for the SNS network to defend against potential anthrax attacks in the U.S. We calibrate our model using multiple literature sources that studied different facets of the problem. Our integrated framework allows us to derive precise prescriptive recommendations to the CDC. We find

that, for example, if the CDC wanted to ensure a 90% survivability target for attacks that simultaneously affect (any) two states, each with at most two cities being attacked, with a detection time of under 48 hours, then the minimum required annual inventory budget would be about $77 million; if the survavibility target were 95%, the budget would amount to roughly $330 million instead. This increasing marginal cost phenomenon, along with other cost/policy characteristics, can be explored quantitatively with the support of our model.

4. *Generalizability*: Our inventory prepositioning problem is qualitatively similar to problems facing supply chain, manufacturing system, or distribution network managers who need to decide on inventory safety stock levels across their networks to protect them from disruptions, in conjunction with inventory re-routing policies, contingent on the one occurred. We illustrate how our framework can capture these problems. We also discuss how our model can be extended to deal with other SNS design problems such as network design or dispensing facilities design.

1.1. Literature Review

Research studies and concerted vaccine distribution effort arising from flu outbreaks or pandemics, *e.g.*, the 2009 H1N1 event, may provide ample experiences, data, and methodological guidance for biodefense research and practice. Indeed, the public health challenges during a pandemic highlight the difficulty of coordinating the distribution of a large amount of vaccines or antibiotics to the public in a timely manner [23]. Flu outbreaks, however, differ from bioattacks in ways that make data and lessons from one type of distribution effort not transferable to the other. First, vaccine distribution for pandemic influenza usually takes place over weeks or months, whereas antibiotic prophylaxis is expected to happen within a handful of days or even hours of a dispensing decision in order to be effective.[2] Second, the infection characteristics of flu dictate that demand is geographically dispersed, whereas anthrax attack could potentially affect entire cities at once. Therefore, an anthrax attack leads to demand patterns that are concentrated both temporally and spatially. This poses a unique strain on the distribution capability of MCMs during a bioattack. In the literature, many works have also focused on drug development in response to the evolution of flu, for example see [50, 16, 38]. From the perspective of pandemic preparedness supply chain research, studies mainly focused on the stochastic behavior of pandemic progression and vaccination strategies over a relatively long period of time and a large space, *e.g.*, see [33, 42, 44, 32]. Moreover, flu outbreaks are random in nature, whereas bioattacks are pre-planned so as to inflict the greatest damage, as

[2] The problem of short treatment time window is exacerbated by the fact that a bioattack is often hard to detect, even if medical tests are actively administered. In fact, even under optimistic medical technology scenarios, expensive tests such as blood donor screening are ineffective in detecting anthrax attacks [25].

we argued above. In this paper, we study the unique properties of bioattacks, such as endogenous and adversarial demand, and their implications on the design of a response supply chain.

Existing research on biodefense supply chain can be broadly categorized into two types. The first type focuses on the detailed design of dispensing strategies immediately after an attack in a metropolitan area [20, 28, 29, 30, 31]. Papers in this stream provide analyses and practical decision support tools that help policymakers determine (optimal) operational parameters for the mass dispensing of antibiotics, advising on key decisions such as the number of Point of Dispenses (POD) to open, modality of the PODs (walk-through, drive-through, and closed), staffing levels, and clinic floor plans. Given the maturity and effectiveness of the decision support tools developed in this stream, we do not repeat effort on this design question. Instead, we work on the multi-stage decision problem that includes prepositioning of inventory in a large (national) network, the uncertainty in demand locations across the network, and the contingent shipment decisions after an attack happens. Since dispensing capacity is exogenous to our model – in the sense that we can capture the variability in dispensing capacity by introducing additional decision variables and cost parameters without losing tractability – our model can be naturally extended to incorporate the learnings from these studies (Section 6).

The second type, which is closer to our work, focuses on the comparison between a small set of prepositioning strategies in anticipation of attacks at specific locations. King and Muckstadt [26, 27] formulate a linear optimization model and a dynamic programming model to evaluate the effectiveness of planned inventory levels on the treatment of patients in a three-echelon tree-like inventory network after bioattacks and influenza outbreaks. Bravata *et al.* [11] evaluate the cost-effectiveness of four alternative supply chain design strategies of maintaining central and distributed inventories to defend against anthrax attacks. Wein *et al.* [47] and Craft *et al.* [17] also developed mathematical models that compare different types of emergency response systems for airborne anthrax attacks. Also for the case of airborne anthrax attacks, the Institute of Medicine in the United States commissioned a book [43] that examines the background and actionable items for prepositioning MCMs to support rapid access to antibiotics. While papers in this stream either focus on the physics of *Bacillus anthracis* dispersion and the details of antibiotic dispensing via a queueing system for a fixed logistical setup, or focus on the evaluation of a particular inventory design strategies, our paper's main focus is on *optimizing* the logistical setup and inventory design, within the policy scope specified by policymakers. We also differ in the level of abstraction: we provide a model that takes the pathogen characteristics (incubation period, infection scale, etc.) as inputs, therefore allowing the model to be calibrated to inform the design of different types of MCM inventory systems. In fact, the ability to stockpile different types of MCMs for more high-priority biothreats has already been a point of discussion for the Strategic National Stockpile program [24].

Aside from bio-preparedness literature, there is a wealth of works in humanitarian logistics that study the prepositioning of disaster relief assets. For comprehensive reviews, we refer the readers to [14, 15, 18]. Recent work by Uichanco [45], which studies the problem of prepositioning disaster relief inventories in anticipation of typhoons in the Philippines, is most similar to ours since it also takes the worst-case approach. A typhoon not only creates demand in the regions it passes through, but potentially also destroys the inventories that are prepositioned at these locations. The author formulates the problem as a two-stage robust optimization problem, providing an exact solution method for the special case of no supply disruption, and a heuristic that samples from the uncertainty set for the general case. Since there is no supply vulnerability in our model, a natural question is whether we can directly employ such an exact solution method. The answer is negative for two reasons. First, in our problem, we focus on the tradeoff between first stage inventory cost and second stage cost that includes demand loss, both of which are absent in [45]. Second, such method leads to a practically intractable formulation in our case since it scales with the number of vertices in the polytope describing the network structure, and a biodefense network typically comprises thousands of nodes and edges.

Our work also relates to papers on manufacturing supply chain design problems in the face of disruptions. Recent papers by Simchi-Levi *et al.* [39, 40] provide a decision support tool to evaluate the performance of manufacturing supply chain under disruptive risks for a given inventory configurations and a given disruption scenario. This is similar to the problem that the Division of SNS Board of Scientific Counselors highlighted in terms of having a quantitative model that can describe the performance of supply chain under shock. Unlike the descriptive nature of these models, ours derives prescriptive suggestions that incorporate two stages of decision making.

The model most similar to ours is the one by Simchi-Levi *et al.* [41], where the authors worked under the setting of a manufacturing supply chain, with the goal of positioning inventories across the network to hedge against capacity disruptions and demand uncertainties. Their focus is on providing an exact solution method. Not surprisingly, this leads to a generally intractable formulation, in particular, a linear optimization problem with an exponentional number of constraints. They propose a novel constraint generation algorithm, which they find to work well in practice for bi-partite graphs involving 200 nodes. However, their constraint generation algorithm still involves the solution of mixed-integer linear optimization problems in its subroutines. Our focus is on providing tractable and scalable (polynomial-time) algorithms, which require the solution only of linear optimization problems. While not being exact for general network topologies, our approach is backed by optimality guarantees under mild assumptions.

On a more abstract level, two-stage resource planning and demand satisfaction problem under the scope of network flow or facility location has been studied in the literature. The work by

Atamtürk and Zhang [5], to our knowledge, was the first to systematically study the two-stage robust network flow problem under demand uncertainty. In particular, the authors study the computational complexity of two-stage network flow problems under budgeted uncertainty sets and find the problem to be intractable in general, except for some special network structures, *e.g.*, a tree structure. In contrast, our focus is not on the characterization of computational complexity, but rather on the derivation of tractable solution approaches. In particular, we study an approximate solution method that gives rise to tractable formulations, and provide strong theoretical and numerical backing for its performance. This also allows us to apply our framework to a practically relevant policy design problem.

Also motivated by bioterrorism events such as the 2001 anthrax attack to postal offices in the U.S., Berman and Gavious [7] study the defender-attacker problem as a min-max facility location problem, where a defender leads with location decisions, and the (strategic) attacker follows with an attack on a single location. The defender can then make a recourse decision to serve the attacked location from the nearest facility. We differ from their work in two ways. First, we allow simultaneous attacks at multiple locations of our network (which is crucial in, for example, anthrax attack preparedness, *cf.* [22]); second, we allow demand loss, and demand is served potentially by multiple stockpile locations in our model, with each stockpile hosting a variable amount of inventory.

An introduction to affine adjustable robust optimization (AARO) is included in Ben-tal *et al.* [6]. There have been a handful of recent results that show AARO heuristics to be optimal under special circumstances [10, 3, 9, 21]. Our works contributes to this stream by providing another optimality proof under a different context. Bertsimas *et al.* [10] studies one-dimensional problems, *e.g.*, inventory problems that involve a single stocking level, while in Delage and Ardestani-Jaafari's work [3], the authors deal with newsvendor type problems under demand uncertainty. We differ from these papers by studying a supply chain network, where the central recourse decision is a multidimensional shipment decision, which is absent in a newsvendor type model. The papers by Iancu *et al.* [21] and Bertsimas *et al.* [9] deal with families of problems, where for optimality (or "good" performance) they require the uncertainty sets to be lattices, or possess a "symmetric" structure. In our model, in order to preclude overly conservative solutions, we rely on simplex-type budget constraints that invalidate both the lattice and the symmetric structures.

2. The Inventory Prepositioning Problem

For exposition purposes, we use SNS to exemplify our discussion of the MCM inventory prepositioning problem. The SNS network is designed to protect the public susceptible to bioattacks in a set of geographic locations, *e.g.*, densely populated towns or neighborhoods, which we shall refer to as *demand* locations. The demand locations are split into administrative divisions according

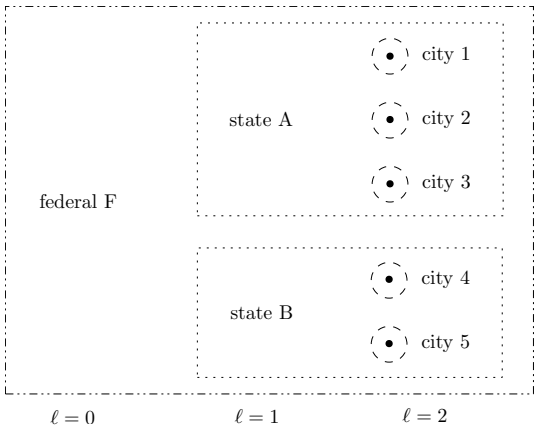

Figure 1 Five demand locations (cities) split into three administrative divisions, federal $\ell = 0$, state $\ell = 1$ and city $\ell = 2$. Note that $\mathcal{P}(1) = \mathcal{P}(2) = \mathcal{P}(3) =$A and $\mathcal{P}(4) = \mathcal{P}(5) =$B; $\mathcal{C}(\text{A}) = \mathcal{D}(\text{A}) = \{1, 2, 3\}$ and $\mathcal{C}(\text{B}) = \mathcal{D}(\text{B}) = \{4, 5\}$; $\mathcal{D}(\text{F}) = \{1, 2, 3, 4, 5\}$.

to a hierarchical structure, *e.g.*, boroughs, municipalities, provinces, states, etc. There are $L + 1$ levels in the hierarchy, indexed by $\ell = 0, \ldots, L$, whereby each division at the lowest (Lth) level comprises precisely one demand location. Divisions at some intermediate ℓth level comprise subsets of divisions at the lower $(\ell + 1)$th level in a nested fashion; the highest (0th) level includes a single division, *e.g.*, federal/national level. For a division i at the ℓth level, let $\mathcal{P}(i)$ be its (unique) parent division at the $(\ell - 1)$th level, $\mathcal{C}(i)$ the set of (children) divisions that it includes at the $(\ell + 1)$th level, and $\mathcal{D}(i)$ the set of demand locations that it includes, *i.e.*,

$$\mathcal{D}(i) = \{\text{demand location } j : \underbrace{\mathcal{P}(\mathcal{P}(\ldots \mathcal{P}(\mathcal{P}}_{L-\ell \text{ times}}(j)) \ldots)) = i\}.$$

Figure 1 includes an illustrative example, where the demand locations are cities, split under state and federal divisions.

To serve the demand locations, each administrative division at the $0, \ldots, L - 1$ levels maintains a *stockpile* of appropriate medical countermeasures. In particular, in case of a bioattack, MCMs would typically need to be shipped from the—usually remotely located—stockpiles to the demand locations to treat the affected population.

Let the demand locations and stockpiles correspond to nodes in a directed graph (V, E), which we refer to as demand and stockpile nodes, respectively. The subset of demand nodes is denoted with V_D. We index the (unique) stockpile node at the highest level division with 0. The edges in E connect stockpile nodes with demand nodes. Specifically, $(i, j) \in E$ if and only if inventory can be shipped from i to $j \in V_D$ once an attack occurs. Shipments have negligible costs and are not subject to capacity constraints for the purposes of the SNS network. However, there is a fixed lead time τ_{ij} for shipping inventory from i to j for all $(i, j) \in E$.

We focus on a particular bioattack threat, in anticipation of which the CDC stores a single type of MCM. Inventory of this MCM can be prepositioned at any node $i \in V$. If i is a demand node, the stored inventory corresponds to predispensed medical kits. We use $\mathbf{x} \in \mathbb{R}^{|V|}$ to denote the amounts of stored inventories allocated at the nodes. The set of all feasible inventory allocations, denoted by $X \subseteq \mathbb{R}^{|V|}$, is assumed to be a polytope. A unit of inventory is adequate to treat precisely one individual. Associated with storing inventory at any node are purchasing, replenishment, maintenance, management costs, etc. We refer to these costs simply as *holding* costs, and denote the per-unit costs with $\mathbf{h} \in \mathbb{R}^{|V|}$. That is, the cost for storing x_i units of MCM at node $i \in V$ is $h_i x_i$.

When an attack takes place, a subset of demand nodes are affected, and parts of their populations are in need of treatment with the MCMs. We also say that division i is affected, if any of its children demand nodes $\mathcal{D}(i)$ is affected. For example, if city 1 is attacked in Figure 1, we say that it is affected and so is state A. Let $\mathbf{d} \in \mathbb{R}^{|V_D|}$ be the (a priori unknown) vector with the realized number of affected individuals in each of the demand nodes. Once $\mathbf{d}$ is revealed, prepositioned inventory at the affected demand nodes is available immediately to treat individuals. In case of shortages, inventory from other nodes can be shipped to satisfy the demands. For each edge $(i,j) \in E$, we use f_{ij} to denote the amount of inventory shipped from i to satisfy demand at node j. Note that the shipment decisions are contingent on the realized demand, which we sometimes make explicit by writing them as $f_{ij}(\mathbf{d})$. Inventory shipped from i would be made available for treatment at node j only after τ_{ij} time units. Delays in treatment of affected population could lead to lower probability of survival. We use $\rho_{ij} \in [0,1]$ to denote the *survival probability* (or survivability) of an individual in node j if treated with inventory shipped from node i, and $\overline{\rho} \in [0,1]$ if left untreated. For example, suppose that node j is affected and 50% of the affected individuals are treated with inventory prepositioned at that node, 30% are treated with inventory shipped from node i, and 20% are left untreated. The *average* survivability would then be $0.5\rho_{jj} + 0.3\rho_{ij} + 0.2\overline{\rho}$.

With respect to the possible attack scenarios, the CDC considers ones involving simultaneous attacks to multiple locations across the country. As a matter of fact, a recent report from an advisory board to the CDC was questioning the current network's ability to respond to three simultaneous attacks [22]. Generalizing this in our framework, we consider attack scenarios (or demand vectors) where, for each administrative division i, at most Γ_i of its children divisions $\mathcal{C}(i)$ are affected. We assume Γ_i's to be non-negative integers and refer to them as the *attack scale* parameters. For example, if the administration levels are states and cities, $\Gamma_i = 2$ for state i would mean that we consider attack scenarios with at most 2 cities in state i being affected.

In case demand location i is affected, the maximum number of individuals in need for treatment at that location is $\hat{d}_i$.[3] A further probabilistic characterization of the possible demand vectors $\mathbf{d}$

[3] The maximum number of affected individuals for a bioattack is estimated by policymakers based on census considerations, *e.g.*, population density, transmission and contagion characteristics, *e.g.*, the required quantity of spores to

appears to be, unfortunately, prohibitive in the CDC's problem for a variety of reasons. One relates to limited historical data, given that bioattacks have so far been rarely encountered in practice. A second, and more important, reason is the nature of terrorist attacks being *adversarial* and *endogenous*, instead of purely random and exogenous. In particular, unlike natural disasters, for instance, bioattacks are pre-meditated and often carefully planned in order to maximize the damage inflicted. The choice of which locations to attack then, which essentially drives the realization of $\mathbf{d}$, is likely to be influenced by the CDC's inventory decisions, given that prepositioned inventory (or lack thereof) is partially visible to the public. Both issues of endogeneity and the adversarial choice of the attacked areas are indeed considered and acknowledged by policymakers [43]. In the next section, we propose a suitable model for $\mathbf{d}$ that addresses these issues, instead of postulating a probabilistic description.

In general, more (less) inventory in the system leads, on the one hand, to higher (lower) holding costs and, on the other hand, to fewer (more) potential casualties. Therefore, CDC needs to balance inventory costs and the costs of life loss. We consider two different ways to navigate this tradeoff, leading to two possible problem formulations:

1. Policymakers explicitly quantify the cost of each life lost to be b monetary units. The CDC's problem is then to select a feasible inventory allocation so as to minimize holding costs plus worst case life loss costs under all possible attack scenarios. We shall refer to this problem formulation as the *Life Loss Cost* (LLC).
2. Policymakers specify survivability targets: let $1-\epsilon_i$ be the target for average survivability in demand node i, for some $\epsilon_i \in [0,1]$, which we shall refer to as the *survivability target* parameters. The CDC's problem is then to select a feasible inventory allocation so as to minimize holding costs, while providing the survivability guarantees implied by the specified targets in all demand locations, under all possible attack scenarios. We shall refer to this problem formulation as the *Life Loss Guarantee* (LLG).

Our model is well-suited for policy decision-making purposes. In particular, the attack scale parameters $\{\Gamma_i : i \in V\}$ allow policymakers to specify the severity of the attacks they want to hedge against, both in terms of their *magnitude*, since higher values of Γ for lower level nodes translate into more areas affected, *e.g.*, cities, and in terms of their *complexity*, since higher values of Γ for higher level nodes translate into the affected areas being dispersed among more divisions, *e.g.*, states. Furthermore, the life loss cost b in the (LLC) formulation, or the survivability target parameters $\{\epsilon_i : i \in V_D\}$ in the (LLG) formulation, reflect the policymakers' aversion to casualties

carry out an attack and their ability to remain aloft and travel further for aerosol attacks, and others. The estimation usually relies on experimental data, see for example our discussion in Section 5.

and insufficient coverage. Based on the policymakers' selections, the model prescribes appropriate inventory prepositioning strategies and elicits their minimum required costs, which allows for tradeoff analyses.

In the rest of the paper, we first propose a tractable solution approach to CDC's problem for both the (LLC) and (LLG) formulations, providing analytical and numerical evidence for its fidelity. We then apply it to a case study of the anthrax SNS inventory prepositioning problem.

3. Formulation and Solution Approach

For both (LLC) and (LLG), we formulate the inventory prepositioning problem as a two-stage robust optimization problem. In particular, at the first stage, the policymaker decides on the prepositioned inventory allocation $\mathbf{x} \in X$. Subsequently, "nature" draws an attack scenario or demand vector $\mathbf{d}$ from the set of scenarios compatible with the specified attack scale parameters, denoted by $U \subset \mathbb{R}^{|V_D|}$, so as to minimize expected survivors. We also refer to U as the demand uncertainty set. Note that the demand vector is selected having observed $\mathbf{x}$ and in anticipation of possible inventory shipment decisions. That is, at the second stage, after the realized demand vector $\mathbf{d} \in U$ is revealed, the policymaker decides on the shipment strategy $\{f_{ij}(\mathbf{d}) : (i,j) \in E\}$ so as to minimize life loss costs in the (LLC) formulation, or to provide sufficient coverage as prescribed by the survivability target parameters in (LLG).

Formally, we model the Life Loss Cost problem as

$$
\begin{aligned}
\text{(LLC):} \quad \min_{\mathbf{x},\, \mathbf{f}(\cdot),\, \mathbf{s}(\cdot)} \quad & \mathbf{h}'\mathbf{x} \;+\; \max_{\mathbf{d} \in U} \; b \sum_{i \in V_D} \left((1-\overline{\rho}) s_i(\mathbf{d}) + \sum_{j:(j,i) \in E} (1-\rho_{ji}) f_{ji}(\mathbf{d}) \right) && \text{(1a)} \\
\text{subject to} \quad & x_i \geq \sum_{j:(i,j) \in E} f_{ij}(\mathbf{d}), \quad \forall i \in V, \forall \mathbf{d} \in U && \text{(1b)} \\
& s_i(\mathbf{d}) + \sum_{j:(j,i) \in E} f_{ji}(\mathbf{d}) = d_i, \quad \forall i \in V_D, \forall \mathbf{d} \in U && \text{(1c)} \\
& \sum_{j:(j,i) \in E} f_{ji}(\mathbf{d}) \leq d_i, \quad \forall i \in V_D, \forall \mathbf{d} \in U && \text{(1d)} \\
& f_{ij}(\mathbf{d}) \geq 0, \quad \forall (i,j) \in E, \forall \mathbf{d} \in U && \text{(1e)} \\
& \mathbf{x} \in X. && \text{(1f)}
\end{aligned}
$$

The auxiliary variables $\{s_i(\cdot) : i \in V_D\}$ capture demand shortages, *i.e.*, the number of affected individuals left untreated at each node. Note that both the shipment decision variables $\mathbf{f}(\cdot)$ and the shortage variables $\mathbf{s}(\cdot)$ are adjustable, contingent on the realized demand vector $\mathbf{d}$. The objective is to minimize inventory holding costs plus worst-case life loss costs. Constraint (1b) is a flow conservation condition: the total amount of inventory shipped from node i should be less than the amount stockpiled at i. Constraint (1c) defines the demand shortage variable s_i for each node i.

Constraint (1d) upperbounds the inventory shipped into and consumed at node i by d_i, since one unit of inventory is used to treat precisely one individual.

Similarly, we formulate (LLG) as follows:

$$\text{(LLG):} \quad \min_{\mathbf{x},\mathbf{f}(\cdot),\mathbf{s}(\cdot)} \quad \mathbf{h}'\mathbf{x} \tag{2a}$$

$$\text{subject to} \quad \overline{\rho} s_i(\mathbf{d}) + \sum_{j:(j,i)\in E} \rho_{ji} f_{ji}(\mathbf{d}) \geq (1-\epsilon_i) d_i, \quad \forall i \in V_D, \forall \mathbf{d} \in U \tag{2b}$$

$$\text{(1b), (1c), (1d), (1e), (1f).} \tag{2c}$$

Compared to (LLC), the (LLG) formulation has an objective of minimizing holding costs, while ensuring that the average survivability at each node is higher than the target set, as reflected by the added constraint (2b). Throughout this paper we assume that $\rho_{ji} \geq \overline{\rho}$ for all $(j,i) \in E$, *i.e.*, treatment increases survivability; and $\overline{\rho} \leq 1-\epsilon_i$ for all $i \in V_D$, otherwise (LLG) reduces to a trivial problem with optimal cost of zero.

We believe that our robust optimization formulations of the SNS inventory prepositioning problem are best-suited to capture the practical considerations facing CDC for the following reasons:

1. *Adversarial & endogenous demand*: Bioattacks are pre-planned and often target locations so as to inflict the greatest damage, in response to preparedness efforts. Our formulations precisely capture this feature by allowing "nature" to adversarially pick a demand vector $\mathbf{d}$ after the inventory allocation $\mathbf{x}$ is decided.
2. *Worst-case guarantees*: Policy decisions related to public safety are usually subject to coverage guarantees that they need to provide. By requiring the prescribed coverage to be achievable under all possible attack scenarios under consideration, see constraint (2b), formulation (LLG) furnishes the desired guarantees. Similarly, (LLC) also minimizes worst-case life loss costs.
3. *Unknown demand*: Bioattack locations are highly unpredictable, because of sparsity, or complete lack of historical data. By relying on a worst-case analysis and modeling the demand via means of an uncertainty set, which requires less data to calibrate in comparison with a distributional probabilistic description, formulations (LLC) and (LLG) hedge against demand uncertainty and provide robust inventory allocation decisions.

From an implementation standpoint, formulations (LLC) and (LLG) admit tractable, scalable solution approaches for dealing with practical networks involving thousands of nodes and edges, which we attend to next, after we provide a formulation for the set of attack scenarios U.

3.1. Set of Attack Scenarios

We provide a formulation for the set of attack scenarios under consideration. In particular, recall that, given some attack scale parameters $\{\Gamma_i : i \in V\}$, a possible scenario involves demand nodes

affected so that, for each administrative division i, no more than Γ_i of its children divisions $\mathcal{C}(i)$ are affected. Consider

$$U := \left\{ \mathbf{d} \in \mathbb{R}^{|V_D|} : \boldsymbol{\xi} \in \mathbb{R}^{|V|},\, d_i = \hat{d}_i \xi_i \,\forall i \in V_D,\, 0 \leq \xi_i \leq \xi_{\mathcal{P}(i)} \,\forall i \in V \setminus \{0\},\, \xi_0 = 1,\, \sum_{j \in \mathcal{C}(i)} \xi_j \leq \Gamma_i \xi_i \,\forall i \in V \right\}.$$

As we will show, only the extreme points of U will be relevant for the optimal solution of (LLC) and (LLG). Therefore, to argue for the correctness of the above formulation for U, it suffices to argue that its extreme points precisely correspond to the attack scenarios under consideration. Indeed, as we will also show, the auxiliary variables $\boldsymbol{\xi}$ are binary at the extreme points of U. Then, they bear the following interpretation: ξ_i indicates whether node i is affected or not. In particular, if i is a demand node,

$$d_i = \begin{cases} \hat{d}_i & \text{if } i \text{ is affected, } \xi_i = 1 \\ 0 & \text{otherwise.} \end{cases}$$

The constraint $\xi_i \leq \xi_{\mathcal{P}(i)}$ enforces all parent divisions of an affected node to also be affected, *i.e.*, $\xi_j = 1$ for all j such that $i \in \mathcal{D}(j)$ and i is affected. Finally, constraint $\sum_{j \in \mathcal{C}(i)} \xi_j \leq \Gamma_i \xi_i$ ensures that, if i is affected, at most Γ_i of its children divisions are affected, as we required. As a side note, it can be readily seen that the set U also includes all remaining attack scenarios that are compatible with the attack scale parameters, but have a number of affected individuals $d_i \leq \hat{d}_i$.

To facilitate exposition, we also let

$$\Xi := \left\{ \boldsymbol{\xi} \in \mathbb{R}^{|V|} : 0 \leq \xi_i \leq \xi_{\mathcal{P}(i)} \,\forall i \in V \setminus \{0\},\, \xi_0 = 1,\, \sum_{j \in \mathcal{C}(i)} \xi_j \leq \Gamma_i \xi_i \,\forall i \in V \right\}.$$

We can then simply express $U = \left\{ \mathbf{d} \in \mathbb{R}^{|V_D|} : d_i = \hat{d}_i \xi_i \,\forall i \in V_D,\, \boldsymbol{\xi} \in \Xi \right\}$.

3.2. Solution Approach

By involving both static, $\mathbf{x}$, and recourse decisions, $\mathbf{f}(\cdot)$, $\mathbf{s}(\cdot)$, formulations (LLC) and (LLG) fall into the class of so-called multi-stage adjustable robust optimization problems (ARO). Problems in that class are, in general, computationally intractable [6], because they require the optimization over functions, or policies, instead of vectors, and this makes them infinite-dimensional problems. Specifically, $\mathbf{f}(\cdot)$ and $\mathbf{s}(\cdot)$ are policies that could take different values contingent on the uncertain parameters' realization (namely, the demand $\mathbf{d}$).

Most popular techniques to deal with ARO problems in the literature are heuristics and constraint/column generation methods. One popular heuristic, which we also adopt to tackle our problem, is to limit attention to policies restricted to depend affinely on the uncertain parameters, which are often referred to as affine policies (AP), as opposed to fully adjustable policies (FP).

This restriction often enables tractability, see, *e.g.*, [6]. In our setting, the affinely adjustable robust counterpart of (LLG), for example, is

$$
\begin{aligned}
\text{(ALLG):} \min_{\mathbf{x},\mathbf{F},\mathbf{S}} \quad & \mathbf{h}'\mathbf{x} && \text{(3a)}\\
\text{subject to} \quad & \overline{\rho}(\mathbf{S}_i'\mathbf{d} + S_i^0) + \sum_{j:(j,i)\in E} \rho_{ji}(\mathbf{F}_{ji}'\mathbf{d} + F_{ji}^0) \geq (1-\epsilon_i)d_i, \quad \forall i \in V_D, \forall \mathbf{d} \in U && \text{(3b)}\\
& x_i \geq \sum_{j:(i,j)\in E} (\mathbf{F}_{ij}'\mathbf{d} + F_{ij}^0), \quad \forall i \in V, \forall \mathbf{d} \in U && \text{(3c)}\\
& (\mathbf{S}_i'\mathbf{d} + S_i^0) + \sum_{j:(j,i)\in E} (\mathbf{F}_{ji}'\mathbf{d} + F_{ji}^0) = d_i, \quad \forall i \in V_D, \forall \mathbf{d} \in U && \text{(3d)}\\
& \sum_{j:(j,i)\in E} (\mathbf{F}_{ji}'\mathbf{d} + F_{ji}^0) \leq d_i, \quad \forall i \in V_D, \forall \mathbf{d} \in U && \text{(3e)}\\
& \mathbf{F}_{ji}'\mathbf{d} + F_{ji}^0 \geq 0, \quad \forall (i,j) \in E, \forall \mathbf{d} \in U && \text{(3f)}\\
& \mathbf{x} \in X, && \text{(3g)}
\end{aligned}
$$

where $\mathbf{F}_{ij} \in \mathbb{R}^{|V_D|}$, $F_{ij}^0 \in \mathbb{R}$ for all $(i,j) \in E$, and $\mathbf{S}_i \in \mathbb{R}^{|V_D|}$, $S_i^0 \in \mathbb{R}$ for all $i \in V_D$ are variables corresponding to the affine policies' coefficients. The affinely adjustable version of (LLC) is of similar form. It can be readily seen that both (ALLC) and (ALLG) can be cast as linear optimization problems. Hence, under the practical assumption that X can be expressed by a small number of constraints, (ALLC) and (ALLG) can be solved efficiently, in a tractable and scalable manner.

On the flipside, tractability of AP heuristics to deal with ARO problems often comes at the cost of suboptimal solutions. In fact, for some AROs, the optimality gap between the objective value under AP and the objective value of the original formulation under FP can grow indefinitely with the dimension of the problem [8]. As we pointed out in the literature review, a handful of papers have recently identified conditions under which AP are indeed optimal. These conditions require the absence of simplex-type constraints in the uncertainty set. In our model, however, the simplex-type constraints $\sum_j \xi_j \leq \Gamma_i \xi_i$ are essential to preclude excessively conservative demand scenarios, where an arbitrary number of nodes are affected. Consequently, given the current state of affairs in the robust optimization literature, the performance of AP heuristics (ALLC) and (ALLG) remains questionable. The next section is devoted to providing evidence that (ALLC) and (ALLG) are indeed likely to produce near-optimal solutions for the original (LLC) and (LLG) formulations, respectively.

4. Optimality of Affine Shipment Policies

We provide evidence that affine policies are near-optimal for our problem formulations (LLC) and (LLG). First, and more importantly, we analytically show that under mild additional assumptions (on the survivability parameters and the network structure), AP are indeed optimal. Second, we

conduct numerical studies illustrating that the suboptimality gap remains small for instances that violate the additional assumptions guaranteeing optimality.

4.1. Optimality Result

Consider the following assumptions.

ASSUMPTION 1. *The survival probabilities under treatment are all equal, i.e.,* $\rho_{ij} = \rho \ \forall (i,j) \in E$.

ASSUMPTION 2. *Stockpiles serve all demand nodes in their division, and only demand nodes in their division, i.e.,* $(i,j) \in E \iff j \in \mathcal{D}(i)$.

Assumption 1 requires that the difference in shipment times between stockpile and demand nodes bears no effect on the survivability of treated individuals. Note that this assumption will be violated for biothreats with incubation periods shorter than the shipment times, *e.g.*, for nerve-agents that require treatment within minutes or hours after an attack [43]. However, it will be satisfied for biothreats with longer incubation periods, *e.g.*, for anthrax attacks that are detected early (see also our discussion in Section 5). Assumption 2 requires that stockpiles, which are maintained by administrative divisions, serve affected locations only within their division. For example, in the U.S., this would mean that the stockpiles maintained by states are reserved for usage by their residents. Let $z^\star_{\text{LLC}}$, $z^\star_{\text{LLG}}$, $z^\star_{\text{ALLC}}$, $z^\star_{\text{ALLG}}$ be the optimal values of formulations (LLC), (LLG), (ALLC), (ALLG) respectively. We have the following result.

THEOREM 1. *Under Assumptions 1 and 2, affine policies are optimal for (LLG), i.e.,*

$$z^\star_{\text{LLG}} = z^\star_{\text{ALLG}}.$$

Furthermore, if $\rho = 1$*, affine policies are optimal for (LLC), i.e.,*

$$z^\star_{\text{LLC}} = z^\star_{\text{ALLC}}.$$

To illustrate the applicability of our methodology beyond the scope of MCM inventory prepositioning, we prove our result in a more general model. In particular, for any node we consider shipments to any of its children nodes, not just its demand (leaf) nodes. Furthermore, we allow demand to occur at any node in V, not just the (leaf) nodes in V_D. We also consider demand vectors that, apart from the unknown component $\hat{d}$, entail a deterministic component $\bar{d}$ that realizes under any scenario, and can be thus thought of as the network's "nominal" demand. In other words, we deal with a more general supply chain network where inventory can be stored at nodes and shipped over the (tree-style) network in order to satisfy nominal demand, plus unknown demand shocks, across the entire network. We formalize this generalization within the proof of Theorem 1 below and show that it subsumes the MCM prepositioning problems (LLC) and (LLG) as special cases. We discuss alternative applications in Section 6.

Proof of Theorem 1. Under Assumption 2, our model can be reformulated to one where, instead of inventory shipments over the edges of (V,E), $\{f_e : e \in E\}$, we consider inventory shipments over the edges of the directed out-tree (V,T) with root node 0 and $T := \{(i,j) : i \in V, j \in \mathcal{C}(i)\}$. This is because, under Assumption 2, any inventory shipment to node j occurs from some "parent node" i such that $j \in \mathcal{D}(i)$, *i.e.*, $\mathcal{P}^{L-\ell}(j) = i$ for some ℓ, where $\mathcal{P}^n(k) := \mathcal{P}(\mathcal{P}^{n-1}(k))$ for n positive integer, $k \in V$ and $\mathcal{P}^0(k) := k$. Thus, any f_{ij} can be thought of as a flow along the unique path $i \to \mathcal{P}^{L-\ell-1}(j) \to \ldots \mathcal{P}(j) \to j$. It can then be readily seen that our model entails a *path-based* network flow formulation for inventory shipments in the graph (V,T). In the rest of the proof, we consider the associated *edge-based* formulation, and denote the shipments over the edges with $\mathbf{y} = \{y_t : t \in T\}$. Clearly, this is without loss, since for every feasible $(\mathbf{f},\mathbf{s})$ in the path-based formulation, there exists $\mathbf{y}$ such that $(\mathbf{y},\mathbf{s})$ is feasible for the edge-based formulation, and vice versa (for more details see Chapter 3.5 in [2]).

Furthemore, we assume that demand occurs at every node; specifically, demand at node i is $d_i = \bar{d}_i + \hat{d}_i \xi_i$ for all $i \in V$ and some $\boldsymbol{\xi} \in \Xi$. Unmet demand at each node in $V \setminus V_D$ is treated in the same way as at nodes in V_D: either penalized at a cost rate b under the (LLC), or subject to a guarantee under the (LLG). Clearly, for $\bar{d}_i = 0$ for all $i \in V$ and $\hat{d}_i = 0$ for all $i \in V \setminus V_D$, we recover our original formulations. Thus, we deal with this more general model without loss.

To prove optimality of affine policies, it suffices to show that for any static inventory allocation decision $\mathbf{x} \in X$, there exist policies that are affine in the uncertain demand for the adjustable decisions and achieve the same worst-case cost under fully-adjustable policies. Thus, we henceforth consider the static inventory allocation decision $\mathbf{x}$ as fixed.

We first deal with the (LLC) formulation. At the end of the proof, we argue how the (LLG) can be cast as a special case of the (LLC) formulation in this setting. Using the edge-based formulation, the more general demand model, and a fixed inventory allocation $\mathbf{x} \in X$, it can be readily seen that when $\rho = 1$, the (LLC) problem is equivalent to (in the sense that they have the same optimal set)[4]

$$
\begin{aligned}
\min_{\mathbf{y}(\cdot),\mathbf{s}(\cdot)} \max_{\boldsymbol{\xi}\in\Xi} \quad & \mathbf{1}'\mathbf{s}(\boldsymbol{\xi}) \\
\text{subject to} \quad & s_i(\boldsymbol{\xi}) + y_{\mathcal{P}(i)i}(\boldsymbol{\xi}) + x_i \geq \sum_{j\in\mathcal{C}(i)} y_{ij}(\boldsymbol{\xi}) + \bar{d}_i + \hat{d}_i\xi_i, \ \forall i \in V, \forall \boldsymbol{\xi} \in \Xi \\
& y_{\mathcal{P}(i)i}(\boldsymbol{\xi}) + x_i \geq \sum_{j\in\mathcal{C}(i)} y_{ij}(\boldsymbol{\xi}), \ \forall i \in V, \forall \boldsymbol{\xi} \in \Xi \\
& \mathbf{y}(\cdot), \mathbf{s}(\cdot) \geq 0,
\end{aligned}
$$

[4] Technically, this means that if $(\mathbf{f},\mathbf{s})$ is optimal for (LLC), then there exists $\mathbf{y}$ such that $(\mathbf{y},\mathbf{s})$ is optimal for the corresponding edge-based formulation, and vice versa.

where $\mathbf{1}$ is the vector of all ones. Let z_{F} be the optimal value of this fully-adjustable formulation. Correspondingly, let z_{A} be the optimal value of its affinely adjustable counterpart, *i.e.*, when we restrict $\mathbf{y}(\cdot)$ and $\mathbf{s}(\cdot)$ to be affine in $\boldsymbol{\xi}$. It suffices then to show that $z_{\mathrm{F}} = z_{\mathrm{A}}$.

We now introduce some useful notation:

- For some index set I, let $\boldsymbol{\xi}_I := \{\xi_i : i \in I\}$ and $\mathrm{proj}_I \Xi := \{\boldsymbol{\xi}_I : \boldsymbol{\xi} \in \Xi\}$.
- Let V^l be the set of nodes at the lth level, *i.e.*, $V^l := \{j \in V : \mathcal{P}^l(j) = 0\}$.
- Let A_i be the set of ancestor nodes of i, *i.e.*, $A_i := \{i, \mathcal{P}(i), \mathcal{P}^2(i), \ldots, 0\}$.
- We will frequently look into subgraphs of (V,T), specifically out-trees rooted at some node $i \in V^l$, denoted by (V_i, T_i), where $V_i := \{j \in V : \mathcal{P}^k(j) = i \text{ for some } k = 0,1,2,\ldots,L-l\}$, and $T_i := \{(k,l) : k \in V_i, l \in \mathcal{C}(k)\}$.
- Let $\mathcal{Q}_i(\xi_i', x_i, \mathbf{x}_{-i})$ by the set of feasible policies for (V_i, T_i), with inventory at node i being x_i, the inventory on $V_i \setminus \{i\}$ being $\mathbf{x}_{-i}$, and the uncertain parameter being ξ_i' at node i, *i.e.*,

$$
\begin{aligned}
\mathcal{Q}_i(\xi_i', x_i, \mathbf{x}_{-i}) := \{\{\mathbf{y}(\cdot), \mathbf{s}(\cdot)\} :\ & \\
& x_i \geq \sum_{j \in \mathcal{C}(i)} y_{ij}(\boldsymbol{\xi}),\ \forall \boldsymbol{\xi} \in \Xi_i \\
& s_i(\boldsymbol{\xi}) + x_i \geq \sum_{j \in \mathcal{C}(i)} y_{ij}(\boldsymbol{\xi}) + \hat{d}_i \xi_i' + \bar{d}_i,\ \forall \boldsymbol{\xi} \in \Xi_i \\
& y_{\mathcal{P}(k)k}(\boldsymbol{\xi}) + x_k \geq \sum_{j \in \mathcal{C}(k)} y_{kj}(\boldsymbol{\xi}),\ \forall k \in V_i \setminus \{i\}, \forall \boldsymbol{\xi} \in \Xi_i \\
& s_k(\boldsymbol{\xi}) + y_{\mathcal{P}(k)k}(\boldsymbol{\xi}) + x_k \geq \sum_{j \in \mathcal{C}(k)} y_{kj}(\boldsymbol{\xi}) + \hat{d}_k \xi_k + \bar{d}_k,\ \forall k \in V_i \setminus \{i\}, \forall \boldsymbol{\xi} \in \Xi_i \\
& \mathbf{y}(\boldsymbol{\xi}), \mathbf{s}(\boldsymbol{\xi}) \geq 0,\ \forall \boldsymbol{\xi} \in \Xi_i\}.
\end{aligned}
$$

where $\Xi_i(\xi_i') := \{\boldsymbol{\xi} \mid \boldsymbol{\xi} \in \Xi, \xi_i = \xi_i'\}$. We use shorthand notation Ξ_i when there is no ambiguity in ξ_i'.

- Let $\Theta_i(\xi_i', \mathbf{s})$ be the worst-case demand loss in (V_i, T_i) under $\xi_i = \xi_i'$ and (feasible) resource allocation policy $\{\mathbf{y}(\cdot), \mathbf{s}(\cdot)\}$, $\Omega_i^F(\xi_i', x_i, \mathbf{x}_{-i})$ be the worst-case demand loss in V_i under $\xi_i = \xi_i'$ with an optimal fully-adjustable policy, and $\mathcal{Q}_i^\star(\xi_i', x_i, \mathbf{x}_{-i})$ be the set of all optimal policies:

$$
\begin{aligned}
\Theta_i(\xi_i', \mathbf{s}) &:= \max_{\boldsymbol{\xi} \in \Xi_i(\xi_i')} \sum_{k \in V_i} s_k(\boldsymbol{\xi}), \\
\Omega_i^F(\xi_i', x_i, \mathbf{x}_{-i}) &:= \min_{\mathbf{y}(\cdot), \mathbf{s}(\cdot)} \Theta_i(\xi_i', \mathbf{s}) \text{ subject to } \{\mathbf{y}(\cdot), \mathbf{s}(\cdot)\} \in \mathcal{Q}_i(\xi_i', x_i, \mathbf{x}_{-i}), \\
\mathcal{Q}_i^\star(\xi_i', x_i, \mathbf{x}_{-i}) &:= \arg\min_{\mathbf{y}(\cdot), \mathbf{s}(\cdot)} \Theta_i(\xi_i', \mathbf{s}) \text{ subject to } \{\mathbf{y}(\cdot), \mathbf{s}(\cdot)\} \in \mathcal{Q}_i(\xi_i', x_i, \mathbf{x}_{-i}).
\end{aligned}
$$

Similarly, we define the affinely-adjustable counterpart $\Omega_i^A(\xi_i', x_i, \mathbf{x}_{-i})$ as the worst-case demand loss in V_i, restricted to $\{\mathbf{y}(\cdot), \mathbf{s}(\cdot)\} \in \mathcal{Q}_i(\xi_i', x_i, \mathbf{x}_{-i})$ and affine.

Using our notation, $z_{\mathrm{F}} = \Omega_0^F(1, x_0, \mathbf{x}_{-0})$ and $z_{\mathrm{A}} = \Omega_0^A(1, x_0, \mathbf{x}_{-0})$. It thus suffices to show that

$$
\Omega_0^F(1, x_0, \mathbf{x}_{-0}) = \Omega_0^A(1, x_0, \mathbf{x}_{-0}). \tag{7}
$$

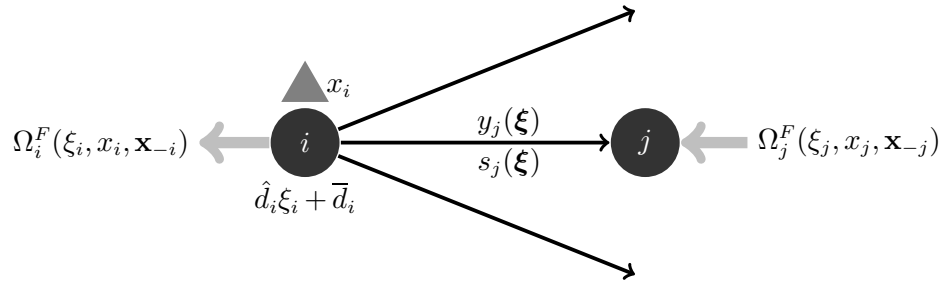

Figure 2 Recursive representation of Ω_i^F.

We now show two useful intermediate results. The first provides a recursive expression for Ω_i^F, and the second shows that Ξ has binary vertices.

PROPOSITION 1. *For all* $i \in V$, $\xi_i' \in [0,1]$, $\mathbf{x} \geq 0$,

$$\Omega_i^F(\xi_i', x_i, \mathbf{x}_{-i}) = \left(\bar{d}_i + \hat{d}_i \xi_i' - x_i + \max_{\boldsymbol{\xi}_{\mathcal{C}(i)} \in \mathrm{proj}_{\mathcal{C}(i)} \Xi_i(\xi_i')} \sum_{j \in \mathcal{C}(i)} \Omega_j^F(\xi_j, x_j, \mathbf{x}_{-j}) \right)^+ .$$

Moreover, $\Omega_i^F(\xi_i, x_i, \mathbf{x}_{-i})$ *is convex in* ξ_i *over* $\xi_i \in [0,1]$.

Proof of Proposition 1. See Appendix A.

Proposition 1 shows the intuitive fact that given a fixed inventory decision and under the optimal policy, the demand shortage in V_i should be the sum of shortages in $\{V_j\}_{j \in \mathcal{C}(i)}$ plus the demand on node i, subtracting away inventory x_i. Based on such recursive definition, we can view the tree as a collection of hub-and-spoke clusters, each consisting of one node and several edges pointing away from this node (Figure 2).

PROPOSITION 2. Ξ *is a polytope with binary vertices,* i.e., $\boldsymbol{\xi} \in ext(\Xi) \implies \boldsymbol{\xi} \in \{0,1\}^n$.

Proof of Proposition 2. See Appendix B.

Now we prove (7) by induction. For a given tree (V_i, T_i) and uncertainty set Ξ_i, we limit our attention to $\{\mathbf{y}(\cdot), \mathbf{s}(\cdot)\}$ that satisfies the following properties:

(I) $\forall m \in V_i$, $j \in \mathcal{C}(m)$, $\boldsymbol{\xi} \in \Xi_i : s_m(\boldsymbol{\xi}) = s_m(\xi_m)$, $y_{mj}(\boldsymbol{\xi}) = y_{mj}(\xi_j)$ are affine in ξ_m, ξ_j respectively.

(II) $\forall m \in V_i$: if $x_m \geq \bar{d}_m + \sum_{j \in \mathcal{C}(m)} \Omega_j^A(0, x_j, \mathbf{x}_{-j})$, then (a) $y_{\mathcal{P}(m)m}(0) = 0$, and (b) $y_{jk}(0) = \Omega_k^A(0, x_k, \mathbf{x}_{-k}) \, \forall (j,k) \in T_m$ and $s_j(0) = 0 \, \forall j \in V_m$.

(III) $\forall m \in V_i$: if $s_m(0) > 0$, then $\forall \boldsymbol{\xi} \in \Xi_i, j \in A_m$, (a) $y_{jk}(\boldsymbol{\xi}) = y_{jk}(0) \, \forall k \in \mathcal{C}(j)$; (b) $y_{\mathcal{P}(j)j}(\boldsymbol{\xi}) + x_j + s_j(\boldsymbol{\xi}) = \sum_{k \in \mathcal{C}(j)} y_{jk}(\boldsymbol{\xi}) + \bar{d}_j + \hat{d}_j \xi_j$; (c) $s_j(\boldsymbol{\xi}) \geq \hat{d}_j \xi_j$.

where we let $y_{\mathcal{P}(i)i}(\boldsymbol{\xi}) := 0$. Properties (II) and (III) describe policies that fulfill deterministic demands as much as possible without over-shipping (Figure 3). Let $V^+(\mathbf{s})$ be the subset of V that contains the nodes i such that $s_i(0) > 0$ and all their ancestor nodes, *i.e.*, $V^+(\mathbf{s}) := \cup_{i : s_i(0) > 0} A_i$. We

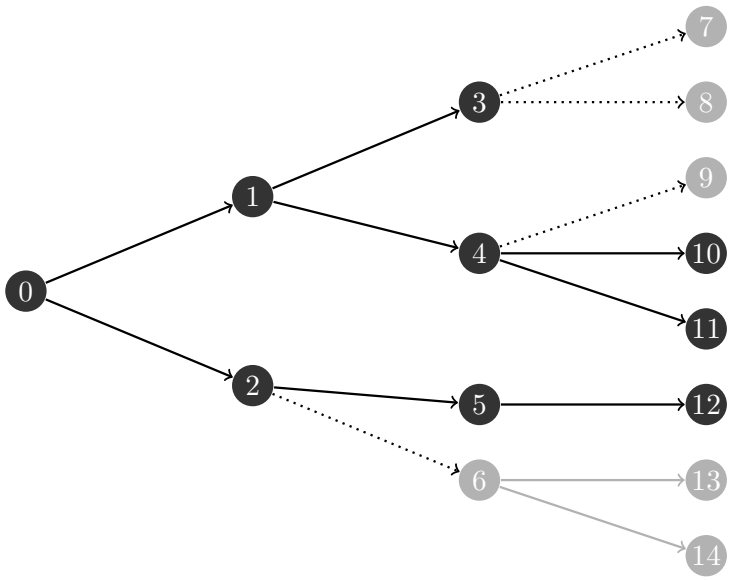

Figure 3 A visual representation of properties (II) and (III) for some out-tree. If the if-condition of (II) is satisfied at nodes 6, 7, 8, and 9, then $y_{37}(\boldsymbol{\xi}) = y_{38}(\boldsymbol{\xi}) = y_{49}(\boldsymbol{\xi}) = y_{26}(\boldsymbol{\xi}) = 0$ for any $\boldsymbol{\xi} \in \Xi_0$, and $s_i(0) = 0 \,\forall i \in V_6 \cup V_7 \cup V_8 \cup V_9$, *i.e.*, deterministic demands on these nodes are fulfilled. If nodes 3, 10, 11, 12 satisfy the if-condition of (III), $V^+(\mathbf{s}) = \{0, 1, 2, 3, 4, 5, 10, 11, 12\}$, and flows on the solid edges are constant and the demand loss constraints are tight for all $\boldsymbol{\xi} \in \Xi_0$.

also let

$$\overline{\mathcal{Q}}_i(\xi_i, x_i, \mathbf{x}_{-i}) := \{\{\mathbf{y}, \mathbf{s}\} \in \mathcal{Q}_i(\xi_i, x_i, \mathbf{x}_{-i}) \,:\, \{\mathbf{y}, \mathbf{s}\} \text{ satisfies (I)-(III)}\}$$
$$\overline{\mathcal{Q}}_i^\star(\xi_i, x_i, \mathbf{x}_{-i}) := \overline{\mathcal{Q}}_i(\xi_i, x_i, \mathbf{x}_{-i}) \cap \mathcal{Q}_i^\star(\xi_i, x_i, \mathbf{x}_{-i}).$$

We are now ready to formalize the induction process.

Induction Hypothesis. If for some $l \in \{0, 1, \ldots, L-1\}$, $\forall j \in V^{l+1}, \mathbf{x} \geq 0$, $\exists\{\bar{\mathbf{y}}^j(\cdot), \bar{\mathbf{s}}^j(\cdot)\}$ such that

$$\text{(Feasibility) } \forall \xi_j \in [0,1], \{\bar{\mathbf{y}}^j(\cdot), \bar{\mathbf{s}}^j(\cdot)\} \in \overline{\mathcal{Q}}_j(\xi_j, x_j, \mathbf{x}_{-j}), \tag{8}$$
$$\text{(Optimality) } \forall \xi_j \in \{0,1\}, \Theta_j(\xi_j, \bar{\mathbf{s}}^j) = \Omega_j^A(\xi_j, x_j, \mathbf{x}_{-j}) = \Omega_j^F(\xi_j, x_j, \mathbf{x}_{-j}), \tag{9}$$

then, $\forall i \in V^l, \mathbf{x} \geq 0$, $\exists\{\bar{\mathbf{y}}^i(\cdot), \bar{\mathbf{s}}^i(\cdot)\}$ such that

$$\text{(Feasibility) } \forall \xi_i \in [0,1], \{\bar{\mathbf{y}}^i(\cdot), \bar{\mathbf{s}}^i(\cdot)\} \in \overline{\mathcal{Q}}_i(\xi_i, x_i, \mathbf{x}_{-i}), \tag{10}$$
$$\text{(Optimality) } \forall \xi_i \in \{0,1\}, \Theta_i(\xi_i, \bar{\mathbf{s}}^i) = \Omega_i^A(\xi_i, x_i, \mathbf{x}_{-i}) = \Omega_i^F(\xi_i, x_i, \mathbf{x}_{-i}). \tag{11}$$

Base Case ($l = L-1$). Given some $\mathbf{x} \geq 0$, for each $j \in V^L$ we define $\bar{s}_j^j(\boldsymbol{\xi}) = \bar{s}_j^j(\xi_j) = \xi_j(\hat{d}_j + \bar{d}_j - x_j)^+ + (1-\xi_j)(\bar{d}_j - x_j)^+$. This policy satisfies (I) by construction. For (II), if $x_j \geq \bar{d}_j$, then $\bar{s}_j^i(0) = (\bar{d}_j - x_j)^+ = 0$. For (III), $\bar{s}_j^j(0) > 0 \implies \bar{s}_j^j(0) = (\bar{d}_j - x_j)^+ > 0 \implies \bar{s}_j^j(0) + x_j = \bar{d}_j$ and $\bar{s}_j^j(1) + x_j = \bar{d}_j + \hat{d}_j$, thus $\bar{s}_j^j(\xi_j) + x_j = \bar{d}_j + \hat{d}_j\xi_j$ and $\bar{s}_j^j(\xi_j) \geq \hat{d}_j\xi_j$. It is straightforward to check that constraints in $\mathcal{Q}_j(\xi_j', x_j, \mathbf{x}_{-j})$ are satisfied under any $\xi_j' \in [0,1]$. For optimality, $\Theta_j(\xi_j' = 0, \bar{s}_j^j) =$

$(\bar{d}_j - x_j)^+ = \Omega_j^F(\xi'_j = 0, x_j, 0)$, $\Theta_j(\xi'_j = 1, \bar{s}_j^j) = (\hat{d}_j + \bar{d}_j - x_j)^+ = \Omega_j^F(\xi'_j = 1, x_j, 0)$. Since $\Theta_j(\xi'_j, \bar{s}_j^j)$ and $\Omega_j^F(\xi'_j, x_j, 0)$ are upper and lower bounds on $\Omega_j^A(\xi'_j, x_j, 0)$, we have that $\forall \xi_j \in \{0,1\}, \Theta_j(\xi_j, \bar{s}_j^j) = (\bar{d}_j + \hat{d}_j \xi_j - x_j)^+ = \Omega_j^A(\xi_j, x_j, 0) = \Omega_j^F(\xi_j, x_j, 0)$.

General Step. Now we prove the general induction step: suppose (8)-(9) hold for some $l \in \{0, 1, \ldots, L-1\}$ and $\forall j \in V^{l+1}, \mathbf{x} \geq 0$. To construct $\{\bar{\mathbf{y}}^i(\cdot), \bar{\mathbf{s}}^i(\cdot)\}$, we define the following. Since $\Omega_j^A(\xi_j, x_j, \mathbf{x}_{-j})$ is nondecreasing in ξ_j and nonnegative, there necessarily exists $g_j, g_j^0 \geq 0$ such that $\Omega_j^A(\xi_j, x_j, \mathbf{x}_{-j}) = g_j \xi_j + g_j^0$ for $\xi_j \in \{0,1\}$. Let $\alpha_i := \min\left(1, \frac{x_i}{\sum_{j \in \mathcal{C}(i)} g_j^0 + \bar{d}_i}\right)$ if $\sum_{j \in \mathcal{C}(i)} g_j^0 + \bar{d}_i > 0$, and $\alpha_i := 1$ otherwise; $\beta_i := \min\left(1, \frac{\left(x_i - \sum_{j \in \mathcal{C}(i)} g_j^0 - \bar{d}_i\right)^+}{\sum_{j=1}^{\Gamma_i} g_{(j)} + \hat{d}_i}\right)$ if $\sum_{j=1}^{\Gamma_i} g_{(j)} + \hat{d}_i > 0$, and $\beta_i := 1$ otherwise, where $g_{(j)}$ is the jth largest element of $\{g_j\}_{j \in \mathcal{C}(i)}$. We can think of α_i as the coverage ratio for deterministic demands in V_i, and β_i as the surge demand coverage ratio.

We are now ready to construct affine $\{\bar{\mathbf{y}}^i, \bar{\mathbf{s}}^i\}$:

$$\{\bar{\mathbf{y}}^i, \bar{\mathbf{s}}^i\} = \begin{cases} \bar{y}_{ij}^i(\xi_j) = \alpha_i g_j^0 + \beta_i g_j \xi_j & \forall j \in \mathcal{C}(i) \\ \bar{s}_i^i(\xi_i) = (1-\alpha_i)\bar{d}_i + (1-\beta_i)\hat{d}_i \xi_i & \\ \bar{y}_{km}^i(\xi_m) = \bar{y}_{km}^{j1}(\xi_m) & \forall (k,m) \in T_j, \forall j \in \mathcal{C}(i) \\ \bar{s}_k^i(\xi_k) = \bar{s}_k^{j0}(0)(1-\xi_k) + \bar{s}_k^{j1}(1)\xi_k & \forall k \in V_i \setminus \{i\}. \end{cases} \tag{12}$$

Let $\overline{\mathcal{Q}}_{j0}^\star := \overline{\mathcal{Q}}_j^\star(0, x_j + \bar{y}_{ij}^i(0), \mathbf{x}_{-j})$ and $\overline{\mathcal{Q}}_{j1}^\star := \overline{\mathcal{Q}}_j^\star(1, x_j + \bar{y}_{ij}^i(1), \mathbf{x}_{-j})$. By the induction hypothesis, $\overline{\mathcal{Q}}_{j0}^\star, \overline{\mathcal{Q}}_{j1}^\star \neq \emptyset$, since $x_j + \bar{y}_{ij}^i(\xi_j) \geq 0$ for $\xi_j \in [0,1]$. We require that $\bar{\mathbf{y}}^{j0}, \bar{\mathbf{s}}^{j0}, \bar{\mathbf{y}}^{j1}$, and $\bar{\mathbf{s}}^{j1}$ satisfy Proposition 3.

PROPOSITION 3. *$\exists \{\bar{\mathbf{y}}^{j0}, \bar{\mathbf{s}}^{j0}\} \in \overline{\mathcal{Q}}_{j0}^\star, \{\bar{\mathbf{y}}^{j1}, \bar{\mathbf{s}}^{j1}\} \in \overline{\mathcal{Q}}_{j1}^\star$ such that $\bar{\mathbf{y}}^{j1}(0) = \bar{\mathbf{y}}^{j0}(0)$ and $\bar{s}_k^{j1}(0) = \bar{s}_k^{j0}(0)$ for all $k \in V_j \setminus \{j\}, j \in \mathcal{C}(i)$.*

Proof for Proposition 3. See Appendix C.

We now check the feasibility and optimality of $\{\bar{\mathbf{y}}^i, \bar{\mathbf{s}}^i\}$.

For (Feasibility), note that Property (I) holds by construction.

To show $\{\bar{\mathbf{y}}^i, \bar{\mathbf{s}}^i\}$ satisfies (II): if $\alpha_i < 1$, $x_i < \bar{d}_i + \sum_{j \in \mathcal{C}(i)} \Omega_j^A(0, x_j, \mathbf{x}_{-j})$, the if-condition in (II) does not hold for node i. For $j \in \mathcal{C}(i)$, if $x_j \geq \bar{d}_j + \sum_{k \in \mathcal{C}(j)} \Omega_k^A(0, x_k, \mathbf{x}_{-k})$, then $g_j^0 = (\bar{d}_j + \sum_{k \in \mathcal{C}(j)} \Omega_k^F(0, x_k, \mathbf{x}_{-k}) - x_j)^+ = (\bar{d}_j + \sum_{k \in \mathcal{C}(j)} \Omega_k^A(0, x_k, \mathbf{x}_{-k}) - x_j)^+ = 0$ by the induction hypothesis, thus $\bar{y}_{ij}^i(0) = 0$; $\bar{y}_{km}^i(0) = \bar{y}_{km}^{j1}(0) = \Omega_m^A(0, x_m, \mathbf{x}_{-m})$, and $\bar{s}_k^i(0) = \bar{s}_k^{j0}(0) = 0$ for $(k,m) \in T_j$ and $k \in V_j$ (both by (II)). For $k \in V_j \setminus \{j\}$, $j \in \mathcal{C}(i)$, (II) holds for $\{\bar{\mathbf{y}}^i, \bar{\mathbf{s}}^i\}$ since (II) holds for $\{\bar{\mathbf{y}}^{j0}, \bar{\mathbf{s}}^{j0}\}$ and $\{\mathbf{y}^{j1}, \mathbf{s}^{j1}\}$. If $\alpha_i = 1$, $\bar{y}_{ij}^i(0) = \alpha_i g_j^0 = g_j^0 = \Omega_j^A(0, x_j, \mathbf{x}_{-j})$; $\bar{y}_{km}^i(0) = \bar{y}_{km}^{j1}(0) = \Omega_m^A(0, x_m, \mathbf{x}_{-m})$ $\forall (k,m) \in T_j, \forall j \in \mathcal{C}(i)$ because $x_i \geq \bar{d}_i + \sum_{j \in \mathcal{C}(i)} \Omega_j^A(0, x_j, \mathbf{x}_{-j})$ and $\{\bar{\mathbf{y}}^{j1}, \bar{\mathbf{s}}^{j1}\}$ satisfies (II); if $x_k \geq \bar{d}_k + \sum_{m \in \mathcal{C}(k)} \Omega_m^A(0, x_m, \mathbf{x}_{-m})$, then $\bar{y}_{\mathcal{P}(k)k}^i(0) = 0$ for any $k \in V_j \setminus \{j\}, j \in \mathcal{C}(i)$ since $\{\bar{\mathbf{y}}^{j1}, \bar{\mathbf{s}}^{j1}\}$ satisfies (II) and $\bar{y}_{\mathcal{P}(k)k}^i(0) = \bar{y}_{\mathcal{P}(k)k}^{j1}(0)$; $\bar{s}_k^i(0) = \bar{s}_k^{j0}(0) = 0$ $\forall k \in V_i \setminus \{i\}$ because $x_i \geq \bar{d}_i + \sum_{j \in \mathcal{C}(i)} \Omega_j^A(0, x_j, \mathbf{x}_{-j})$ and $\{\bar{\mathbf{y}}^{j0}, \bar{\mathbf{s}}^{j0}\}$ satisfies (II); $\bar{s}_i^i(0) = (1-\alpha_i)\bar{d}_i = 0$. Therefore, $\{\bar{\mathbf{y}}^i, \bar{\mathbf{s}}^i\}$ satisfies (II).

To show $\{\bar{\mathbf{y}}^i, \bar{\mathbf{s}}^i\}$ satisfies (III), we again look at the conditions on different sets of nodes separately. If $\alpha_i < 1$, for i, $\bar{s}^i_i(\xi_i) = (1-\alpha_i)\bar{d}_i + \hat{d}_i\xi_i \geq \hat{d}_i\xi_i$, satisfying (IIIc); $\bar{y}^i_{ij}(\xi_j) = \alpha_i g^0_j + 0 = \bar{y}^i_{ij}(0)$, satisfying (IIIa); $x_i + \bar{s}^i_i(\xi_i) = x_i + (1-\alpha_i)\bar{d}_i + \hat{d}_i\xi_i = \alpha_i(\bar{d}_i + \sum_{j\in\mathcal{C}(i)} g^0_j) + \bar{d}_i - \alpha_i\bar{d}_i + \hat{d}_i\xi_i = \sum_{j\in\mathcal{C}(i)} \bar{y}^i_{ij}(\xi_j) + \bar{d}_i + \hat{d}_i\xi_i$ for all $\boldsymbol{\xi} \in \Xi_i$, satisfying (IIIb). For $j \in \mathcal{C}(i)$, $k \in V_j$, $(k,m) \in T_j$, since $\bar{y}^i_{km}(\xi_m) = \bar{y}^{j1}_{km}(\xi_m)$ and $\bar{s}^i_k(\xi_k) = (1-\xi_k)\bar{s}^{j0}_k(0) + \xi_k\bar{s}^{j1}_k(1)$, property (III) holds. If $\alpha_i = 1$, the if-condition of property (III) does not hold, there is nothing to check.

To show $\{\bar{\mathbf{y}}^i, \bar{\mathbf{s}}^i\}$ satisfies the constraints in $\mathcal{Q}_i(\xi'_i, x_i, \mathbf{x}_{-i})$, note that the constraints involving node i are satisfied by construction of $\{\bar{\mathbf{y}}^i, \bar{\mathbf{s}}^i\}$. For nodes downstream from i, note that $\bar{y}^i_{km}(\xi_m) = \bar{y}^{j0}_{km}(0)(1-\xi_m) + \bar{y}^{j1}_{km}(1)\xi_m$ and $\bar{s}^i_k(\xi_k) = \bar{s}^{j0}_k(1-\xi_k) + \bar{s}^{j1}_k(1)\xi_k$, for all $(k,m) \in T_j, j \in \mathcal{C}(i)$ and $k \in V_i \setminus \{i\}$. Since $\{\bar{\mathbf{y}}^{j0}(\cdot), \bar{\mathbf{s}}^{j0}(\cdot)\}$ and $\{\bar{\mathbf{y}}^{j1}(\cdot), \bar{\mathbf{s}}^{j1}(\cdot)\}$ satisfy the constraints of $\mathcal{Q}_j(0, x_j + \bar{y}^i_{ij}(0), \mathbf{x}_{-j})$ and $\mathcal{Q}_j(1, x_j + \bar{y}^i_{ij}(1), \mathbf{x}_{-j})$ respectively, it is straightforward to check the constraint satisfaction of $\{\mathbf{y}^i, \mathbf{s}^i\}$ for $\mathcal{Q}_i(\xi'_i, x_i, \mathbf{x}_{-i})$.

For (Optimality), note that for $\xi'_i \in \{0,1\}$ we have

$$\Theta_i(\xi'_i, \bar{\mathbf{s}}^i) = \bar{s}^i_i(\xi'_i) + \max_{\boldsymbol{\xi}\in\Xi_i} \sum_{j\in\mathcal{C}(i)} \sum_{k\in V_j} \bar{s}^i_k(\xi_k) \tag{13a}$$

$$= \bar{s}^i_i(\xi'_i) + \max_{\substack{\boldsymbol{\xi}_{\mathcal{C}(i)}: \mathbf{1}'\boldsymbol{\xi}_{\mathcal{C}(i)} \leq \Gamma_i\xi'_i \\ \xi_j\in[0,\xi'_i], j\in\mathcal{C}(i)}} \max_{\substack{\boldsymbol{\xi}\in\Xi_j(\xi_j) \\ j\in\mathcal{C}(i)}} \sum_{j\in\mathcal{C}(i)} \sum_{k\in V_j} \bar{s}^i_k(\xi_k) \tag{13b}$$

$$= \bar{s}^i_i(\xi'_i) + \max_{\substack{\boldsymbol{\xi}_{\mathcal{C}(i)}: \mathbf{1}'\boldsymbol{\xi}_{\mathcal{C}(i)} \leq \Gamma_i\xi'_i \\ \xi_j\in[0,\xi'_i], j\in\mathcal{C}(i)}} \sum_{j\in\mathcal{C}(i)} \max_{\boldsymbol{\xi}\in\Xi_j(\xi_j)} \sum_{k\in V_j} \bar{s}^i_k(\xi_k) \tag{13c}$$

$$= \bar{s}^i_i(\xi'_i) + \max_{\substack{\boldsymbol{\xi}_{\mathcal{C}(i)}: \mathbf{1}'\boldsymbol{\xi}_{\mathcal{C}(i)} \leq \Gamma_i\xi'_i \\ \xi_j\in[0,\xi'_i], j\in\mathcal{C}(i)}} \sum_{j\in\mathcal{C}(i)} \max_{\boldsymbol{\xi}\in\Xi_j(\xi_j)} \sum_{k\in V_j} \left\{\bar{s}^{j0}_k(0)(1-\xi_k) + \bar{s}^{j1}_k(1)\xi_k\right\} \tag{13d}$$

$$= \bar{s}^i_i(\xi'_i) + \max_{\substack{\boldsymbol{\xi}_{\mathcal{C}(i)}: \mathbf{1}'\boldsymbol{\xi}_{\mathcal{C}(i)} \leq \Gamma_i\xi'_i \\ \xi_j\in\{0,\xi'_i\}, j\in\mathcal{C}(i)}} \sum_{j\in\mathcal{C}(i)} \max_{\boldsymbol{\xi}\in\Xi_j(\xi_j)} \sum_{k\in V_j} \left\{\bar{s}^{j0}_k(0)(1-\xi_k) + \bar{s}^{j1}_k(1)\xi_k\right\} \tag{13e}$$

$$= \bar{s}^i_i(\xi'_i) + \max_{\substack{\boldsymbol{\xi}_{\mathcal{C}(i)}: \mathbf{1}'\boldsymbol{\xi}_{\mathcal{C}(i)} \leq \Gamma_i\xi'_i \\ \xi_j\in\{0,\xi'_i\}, j\in\mathcal{C}(i)}} \sum_{j\in\mathcal{C}(i)} \Omega^A_j(\xi_j, x_j + \bar{y}^i_{ij}(\xi_j), \mathbf{x}_{-j}) \tag{13f}$$

$$= \bar{s}^i_i(\xi'_i) + \max_{\substack{\boldsymbol{\xi}_{\mathcal{C}(i)}: \mathbf{1}'\boldsymbol{\xi}_{\mathcal{C}(i)} \leq \Gamma_i\xi'_i \\ \xi_j\in\{0,\xi'_i\}, j\in\mathcal{C}(i)}} \sum_{j\in\mathcal{C}(i)} \Omega^F_j(\xi_j, x_j + \bar{y}^i_{ij}(\xi_j), \mathbf{x}_{-j}) \tag{13g}$$

$$= \bar{s}^i_i(\xi'_i) + \max_{\substack{\boldsymbol{\xi}_{\mathcal{C}(i)}: \mathbf{1}'\boldsymbol{\xi}_{\mathcal{C}(i)} \leq \Gamma_i\xi'_i \\ \xi_j\in\{0,\xi'_i\}, j\in\mathcal{C}(i)}} \sum_{j\in\mathcal{C}(i)} \left(\Omega^F_j(\xi_j, x_j, \mathbf{x}_{-j}) - \bar{y}^i_{ij}(\xi_j)\right)^+ \tag{13h}$$

$$= \bar{s}^i_i(\xi'_i) + \max_{\substack{\boldsymbol{\xi}_{\mathcal{C}(i)}: \mathbf{1}'\boldsymbol{\xi}_{\mathcal{C}(i)} \leq \Gamma_i\xi'_i \\ \xi_j\in\{0,\xi'_i\}, j\in\mathcal{C}(i)}} \left(\sum_{j\in\mathcal{C}(i)} \Omega^F_j(\xi_j, x_j, \mathbf{x}_{-j}) - \sum_{j\in\mathcal{C}(i)} \bar{y}^i_{ij}(\xi_j)\right) \tag{13i}$$

$$= \left(\bar{d}_i + \hat{d}_i\xi'_i - x_i + \max_{\substack{\boldsymbol{\xi}_{\mathcal{C}(i)}: \mathbf{1}'\boldsymbol{\xi}_{\mathcal{C}(i)} \leq \Gamma_i\xi'_i \\ \xi_j\in\{0,\xi'_i\}, j\in\mathcal{C}(i)}} \sum_{j\in\mathcal{C}(i)} \Omega^F_j(\xi_j, x_j, \mathbf{x}_{-j})\right)^+ \tag{13j}$$

$$= \left(\bar{d}_i + \hat{d}_i \xi'_i - x_i + \max_{\substack{\boldsymbol{\xi}_{\mathcal{C}(i)}: \mathbf{1}'\boldsymbol{\xi}_{\mathcal{C}(i)} \leq \Gamma_i \xi'_i \\ \xi_j \in [0, \xi'_i], j \in \mathcal{C}(i)}} \sum_{j \in \mathcal{C}(i)} \Omega_j^F(\xi_j, x_j, \mathbf{x}_{-j}) \right)^+ \tag{13k}$$

$$= \Omega_i^F(\xi'_i, x_i, \mathbf{x}_{-i}) = \Omega_i^A(\xi'_i, x_i, \mathbf{x}_{-i}). \tag{13l}$$

Equalities (13a-13d) are straightforward applications of definitions of Θ_i and $\bar{\mathbf{s}}^i$.

To show equality (13e), we argue that is it sufficient to check $\xi_j = 1$ and $\xi_j = 0$ for $j \in \mathcal{C}(i)$. Suppose that $\Xi_j(\xi_j)$ has n extreme points $\boldsymbol{\xi}^1, \ldots, \boldsymbol{\xi}^n$, and $W_m = \{k \in V_j : \xi_k^m = \xi_j\}$, $\overline{W}_m = V_j \setminus W_m$. Since for each extreme point, ξ_k takes value of either ξ_j or 0 (*cf.* Proposition 2), we can write

$$\max_{\boldsymbol{\xi} \in \Xi_j(\xi_j)} \sum_{k \in V_j} \left\{ \bar{s}_k^{j0}(0)(1 - \xi_k) + \bar{s}_k^{j1}(1)\xi_k \right\} = \max_{m \in \{1, \ldots, n\}} \sum_{k \in V_j} \left\{ \bar{s}_k^{j0}(0)(1 - \xi_j)\mathbb{1}_{k \in \overline{W}_m} + \bar{s}_k^{j1}(1)\xi_k \mathbb{1}_{k \in W_m} \right\},$$

which is a convex function of ξ_j ($\mathbb{1}_{i \in I} = 1$ if $i \in I$ and 0 otherwise). By this token, we can replace $\boldsymbol{\xi}_{\mathcal{C}(i)} \in \text{proj}_{\mathcal{C}(i)} \Xi_i$ with $\boldsymbol{\xi}_{\mathcal{C}(i)} \in \text{proj}_{\mathcal{C}(i)} \Xi_i \cap \{0, 1\}^{|\mathcal{C}(i)|}$ for the argument of the outer maximization, since $\Xi_i(0)$ and $\Xi_i(1)$ have binary vertices.

To show equality (13f), note that for $\xi_j = 1$, $\Omega_j^A(1, x_j + \bar{y}_{ij}^i(1), \mathbf{x}_{-j}) = \Theta_j(1, \bar{\mathbf{s}}^{j1}) = \bar{s}_j^{j1}(1) + \max_{\boldsymbol{\xi} \in \Xi_j(1)} \sum_{k \in V_j \setminus \{j\}} \bar{s}_k^{j1}(\xi_k)$, which is equal to $\max_{\boldsymbol{\xi} \in \Xi_j(1)} \sum_{k \in V_j} \bar{s}_k^{j0}(0)(1 - \xi_k) + \bar{s}_k^{j1}(1)\xi_k$ by Proposition 3. For $\xi_j = 0$, $\Omega_j^A(0, x_j + \bar{y}_{ij}^i(0), \mathbf{x}_{-j}) = \Theta_j(0, \bar{\mathbf{s}}^{j0}) = \max_{\boldsymbol{\xi} \in \Xi_j(0)} \sum_{k \in V_j} \bar{s}_k^{j0}(0) = \max_{\boldsymbol{\xi} \in \Xi_j(0)} \sum_{k \in V_j} \bar{s}_k^{j0}(0)(1 - \xi_k) + \bar{s}_k^{j1}(1)\xi_k$.

Equality (13g) holds by the induction hypothesis. Equality (13h) follows from the definition of Ω_j^F and (18).

For equality (13i), by the definitions of α_i and β_i, we have $\beta_i > 0 \implies \alpha_i = 1$, or equivalently, $\alpha_i < 1 \implies \beta_i = 0$. For the subtraction expression inside the brackets in line (13h), one of these two cases is true:

1. $\alpha_i < 1 \implies \Omega_j^F(\xi_j, x_j, \mathbf{x}_{-j}) - \bar{y}_{ij}^i(\boldsymbol{\xi}) = g_j \xi_j + (1 - \alpha_i) g_j^0 \geq 0, \forall j \in \mathcal{C}(i)$, or
2. $\alpha_i = 1 \implies \Omega_j^F(\xi_j, x_j, \mathbf{x}_{-j}) - \bar{y}_{ij}^i(\boldsymbol{\xi}) = (1 - \beta_i) g_j \xi_j \geq 0, \forall j \in \mathcal{C}(i)$.

Both cases lead to the fact that $(\Omega_j^A(\xi_j, x_j, \mathbf{x}_{-j}) - \bar{y}_{ij}^i(\xi_j)) \geq 0$ for $j \in \mathcal{C}(i)$, therefore we can rewrite (13h) into (13i).

For the transition into (13j), consider $\xi'_i = 0$ and $\xi'_i = 1$ separately.

If $\xi'_i = 0$, then $\bar{s}_i^i(0) = (1 - \alpha_i)\bar{d}_i$, $\bar{y}_{ij}^i(0) = \alpha_i g_j^0$, and $\Omega_j^A(0, x_j, \mathbf{x}_{-j}) = g_j^0$,

$$\implies (13\text{i}) = (1 - \alpha_i)\bar{d}_i + \sum_{j \in \mathcal{C}(i)} (1 - \alpha_i) g_j^0 = (1 - \alpha_i) \left(\bar{d}_i + \sum_{j \in \mathcal{C}(i)} g_j^0 \right)$$

$$= \frac{\left((\bar{d}_i + \sum_{j \in \mathcal{C}(i)} g_j^0) - x_i \right)^+}{\bar{d}_i + \sum_{j \in \mathcal{C}(i)} g_j^0} \left(\bar{d}_i + \sum_{j \in \mathcal{C}(i)} g_j^0 \right) = \left(\bar{d}_i + \sum_{j \in \mathcal{C}(i)} g_j^0 - x_i \right)^+ = (13\text{j}).$$

Otherwise if $\xi_i' = 1$, $\bar{s}_i^i(1) = (1-\alpha_i)\bar{d}_i + (1-\beta_i)\hat{d}_i$, $\bar{y}_{ij}^i(\xi_j) = \alpha_i g_j^0 + \beta_i g_j \xi_j$.

For the case of $\alpha_i < 1$ (and consequently $\beta_i = 0$),

$$\begin{aligned}
(13\text{i}) &= (1-\alpha_i)\bar{d}_i + \hat{d}_i + \max_{\boldsymbol{\xi}_{\mathcal{C}(i)} \in \text{proj}_{\mathcal{C}(i)} \Xi_i(1)} \left(\sum_{j \in \mathcal{C}(i)} (1-\alpha_i) g_j^0 + g_j \xi_j \right) \\
&= \bar{d}_i + \hat{d}_i - \alpha_i \bar{d}_i - \alpha_i \sum_{j \in \mathcal{C}(i)} g_j^0 + \max_{\boldsymbol{\xi}_{\mathcal{C}(i)} \in \text{proj}_{\mathcal{C}(i)} \Xi_i(1)} \sum_{j \in \mathcal{C}(i)} (g_j^0 + g_j \xi_j) \qquad \text{(collecting terms)} \\
&= \bar{d}_i + \hat{d}_i - x_i + \max_{\boldsymbol{\xi}_{\mathcal{C}(i)} \in \text{proj}_{\mathcal{C}(i)} \Xi_i(1)} \sum_{j \in \mathcal{C}(i)} \Omega_j^F(\xi_j, x_j, \mathbf{x}_{-j}) \qquad (\alpha_i < 1) \\
&= (13\text{j}).
\end{aligned}$$

For the case of $\alpha_i = 1$ (implying $x_i \geq \sum_{j \in \mathcal{C}(i)} g_j^0 + \bar{d}_i$),

$$\begin{aligned}
(13\text{i}) &= (1-\beta_i)\hat{d}_i + \max_{\boldsymbol{\xi}_{\mathcal{C}(i)} \in \text{proj}_{\mathcal{C}(i)} \Xi_i(1)} \sum_{j \in \mathcal{C}(i)} ((1-\beta_i) g_j \xi_j) \\
&= (1-\beta_i) \left(\hat{d}_i + \max_{\boldsymbol{\xi}_{\mathcal{C}(i)} \in \text{proj}_{\mathcal{C}(i)} \Xi_i(1)} \sum_{j \in \mathcal{C}(i)} g_j \xi_j \right) \qquad \text{(factorization)} \\
&= \frac{\left(\hat{d}_i + \sum_{j=1}^{\Gamma_i} g_{(j)} - (x_i - \sum_{j \in \mathcal{C}(i)} g_j^0 - \bar{d}_i) \right)^+}{\hat{d}_i + \sum_{j=1}^{\Gamma_i} g_{(j)}} \left(\hat{d}_i + \sum_{j=1}^{\Gamma_i} g_{(j)} \right) \qquad (x_i \geq \sum_{j \in \mathcal{C}(i)} g_j^0 + \bar{d}_i) \\
&= \left(\hat{d}_i + \sum_{j=1}^{\Gamma_i} g_{(j)} - (x_i - \sum_{j \in \mathcal{C}(i)} g_j^0 - \bar{d}_i) \right)^+ = (13\text{j}).
\end{aligned}$$

Lastly, (13k) holds by the convexity property of $\sum_{j \in \mathcal{C}(i)} \Omega_j^F(\xi_j, x_j, \mathbf{x}_{-j})$ and (13l) holds by the recursive property, both shown in Proposition 1. We have now completed the proof for the inductive step, thus showing $z_{\text{F}} = z_{\text{A}}$.

To complete the proof, we now turn our attention to the (LLG) formulation. By solving for $s_i(\mathbf{d})$ from (1c) and substituting in (2b), we can eliminate (1c) and re-write (2b) as

$$\sum_{j:(j,i) \in E} f_{ji}(\mathbf{d}) \geq \frac{1 - \epsilon_i - \overline{\rho}}{\rho - \overline{\rho}} d_i, \quad \forall i \in V, \forall \mathbf{d} \in U.$$

At optimality, the above constraint can be taken to be active without loss (if it is not, we can scale down the associated flows into i so that it becomes active). Thus, the (LLG) is equivalent to

$$\begin{aligned}
\min_{\mathbf{x}, \mathbf{f}(\cdot), \mathbf{s}(\cdot)} \quad & \mathbf{h}'\mathbf{x} \\
\text{subject to} \quad & x_i \geq \sum_{j:(i,j) \in E} f_{ij}(\mathbf{d}), \quad \forall i \in V, \forall \mathbf{d} \in U' \\
& s_i(\mathbf{d}) + \sum_{j:(j,i) \in E} f_{ji}(\mathbf{d}) = d_i, \quad \forall i \in V, \forall \mathbf{d} \in U'
\end{aligned}$$

$$
\begin{aligned}
& s_i(\mathbf{d}) = 0, \quad \forall i \in V, \forall \mathbf{d} \in U' \\
& f_{ij}(\mathbf{d}) \geq 0, \quad \forall (i,j) \in E, \forall \mathbf{d} \in U' \\
& \mathbf{x} \in X,
\end{aligned}
$$

where $U' := \left\{ \mathbf{d}' : d'_i = \frac{1-\epsilon_i-\overline{\rho}}{\rho-\overline{\rho}} d_i \, \forall i \in V, \, \mathbf{d} \in U \right\}$. Then, this is in turn equivalent to

$$
\begin{aligned}
\min_{\mathbf{x}, \mathbf{f}(\cdot), \mathbf{s}(\cdot)} \quad \mathbf{h}'\mathbf{x} \quad + \quad \max_{\mathbf{d} \in U'} \quad & b' \sum_{i \in V} (1-\overline{\rho}) s_i(\mathbf{d}) \\
\text{subject to} \quad & x_i \geq \sum_{j:(i,j) \in E} f_{ij}(\mathbf{d}), \quad \forall i \in V, \forall \mathbf{d} \in U' \\
& s_i(\mathbf{d}) + \sum_{j:(j,i) \in E} f_{ji}(\mathbf{d}) = d_i, \quad \forall i \in V, \forall \mathbf{d} \in U' \\
& \sum_{j:(j,i) \in E} f_{ji}(\mathbf{d}) \leq d_i, \quad \forall i \in V, \forall \mathbf{d} \in U' \\
& f_{ij}(\mathbf{d}) \geq 0, \quad \forall (i,j) \in E, \forall \mathbf{d} \in U' \\
& \mathbf{x} \in X
\end{aligned}
$$

for b' large enough. However, this corresponds to an (LLC) instance that satisfies our assumptions and therefore admits an optimal affine adjustable policy. $\square$

4.2. Performance of Affine Policies for the General Case

To quantify the suboptimality gap of the AP heuristics for the general case, we conducted two numerical studies where we sequentially relaxed the optimality-guaranteeing Assumptions 1 and 2. For brevity, we present our studies for the (LLC) formulation—our studies on the (LLG) formulation yielded quantitatively similar results. All our studies consider small-sized networks that allow us to solve the fully-adjustable formulations. The conclusion from both studies below is that the AP heuristic maintains a near-optimal performance: average suboptimality gaps were less than 0.01% and always smaller than 1% in all our experiments.

Study 1. We relax Assumption 1 and allow the survival probabilities to take different values. Specifically, we consider a network of 21 nodes with three administrative levels: node 0 is at the 0th level, nodes 1-4 are at the 1st level, and the remaining nodes are at the 2nd level. Each of the level 1 nodes has 4 children demand nodes. For the 0th node, the attack scale parameter equals 2; for nodes 1-4, they equal 1, 2, 2, and 3, respectively. Life loss cost is $b = 100$. The survival probabilities are randomly sampled between 0.6 and 1, with shipments from nodes higher in the hierarchy corresponding to lower probabilities. Demand shocks $\hat{d}$ are randomly drawn between 0 and 1000. Inventory holding costs at each node are randomly sampled between 1 and 50, with nodes

	$\frac{z^\star_{\text{ALLC}} - z^\star_{\text{LLC}}}{z^\star_{\text{LLC}}}$
average	0.01%
stdev	0.03%
max	0.51%

Table 1 Suboptimality gaps of the affine relaxation in Study 1.

higher in the hierarchy having lower costs. Table 1 reports statistics for the relative suboptimality gap, $(z^\star_{\text{ALLC}} - z^\star_{\text{LLC}})/z^\star_{\text{LLC}}$, we measured over 1,450 generated instances.

To further evaluate the quality of solutions produced by (ALLC) compared with (LLC), we performed experiments where we first fix the first-stage inventory allocation decision, as prescribed by either formulation, and then measure the objective cost under non-worst-case, randomly sampled demand realizations (within U), for which optimal shipping decisions are made. This experimental setup mimics practice more closely, as the re-optimization of shipment decisions in the second stage can always be conducted from an implementation standpoint. Let $z_{\text{LLC}}(\mathbf{d})$ and $z_{\text{ALLC}}(\mathbf{d})$ be the optimal costs from such an approach, when the first-stage inventory allocation is derived using (LLC) and (ALLC), respectively, and the sampled demand vector is $\mathbf{d}$. A histogram of the cost differential, $(z_{\text{ALLC}}(\mathbf{d}) - z_{\text{LLC}}(\mathbf{d}))/z_{\text{LLC}}(\mathbf{d})$, we measured over 55,000 generated instances, and a scatterplot of the actual costs $z_{\text{LLC}}(\mathbf{d})$, $z_{\text{ALLC}}(\mathbf{d})$, are depicted in Figure 4.

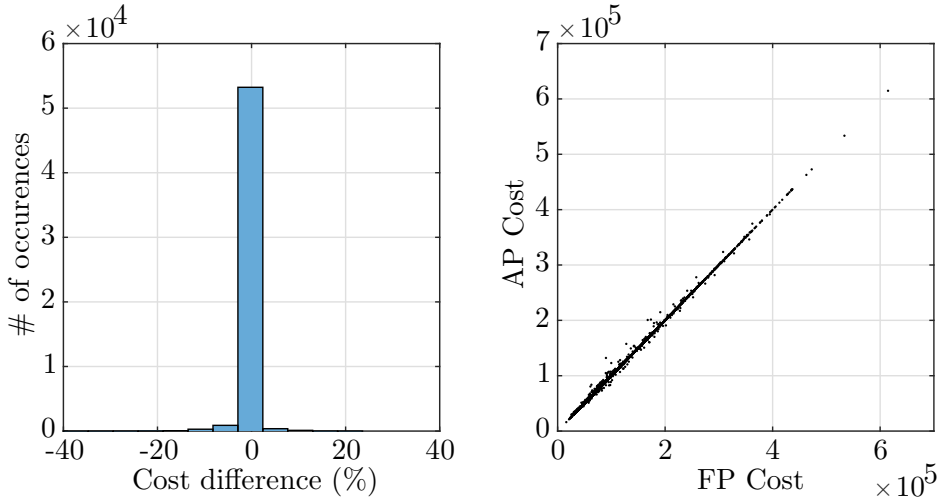

Figure 4 Cost comparison between affine and fully adjustable inventory decisions in Study 1.

Study 2. We now relax Assumption 2 as well. To allow stockpile nodes to serve demand locations outside their administrative divisions, we add the following edges between stockpile nodes and demand nodes: node 2 can serve the children of nodes 3, 4; node 3 can serve the children of 4,

5, etc. All other parameters remain as in Study 1. Table 2 reports statistics for the suboptimality gaps we measured over 850 generated instances. Figure 5 depicts the histogram and scatterplot of costs under random non-worst-case demand scenarios and re-optimization of shipping decisions for 145,000 generated instances (as outlined above).

	$\frac{z^\star_{\text{ALLC}} - z^\star_{\text{LLC}}}{z^\star_{\text{LLC}}}$
average	0.01%
stdev	0.05%
max	0.79%

Table 2 Suboptimality gaps of the affine relaxation in Study 2.

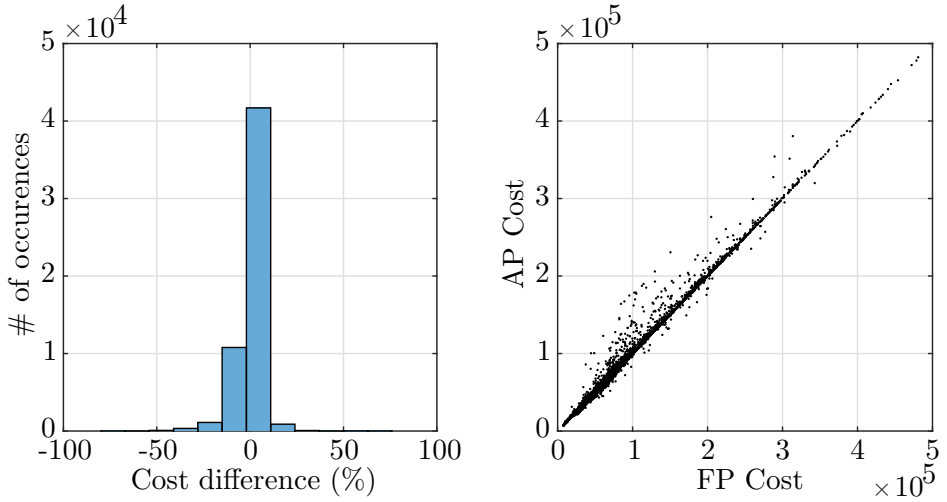

Figure 5 Cost comparison between affine and fully adjustable inventory decisions in Study 2.

5. Strategic National Stockpile Inventory Prepositioning for Anthrax Attacks

In this section, we apply our work in a case study on MCM inventory prepositioning for aerosolized *Bacillus anthracis* (anthrax) attacks in the U.S. We focus on anthrax attacks as they are of particular interest to public health experts because of their relatively high probability of occurrence and potentially devastating impact. To elaborate on this, anthrax cultures are easily obtainable worldwide, and anthrax spores are extremely robust in that they can stay dormant and alive for decades, which allows them to be weaponized and transported securely in a number of forms [43]. Availability and robustness of anthrax weapons increase the likelihood of anthrax attacks. Furthermore, anthrax spores spread easily in the air to affect a large number of people through inhalation. Fatality rate among infected population is high if left untreated for even just a few days.

More precisely, if t is the time between infection and treatment, then, according to the studies of [13, 12, 48, 49], the survival probability $\rho(t)$ of anthrax infected population can be approximated, for $t \leq 200$ hours, by

$$\rho(t) = e^{-(0.004t)^2}. \tag{16}$$

Considering the time it would take to detect an anthrax attack and the time to ship the MCMs from a regional warehouse to individuals, which is likely to be on the order of days [43], CDC is exploring different options in prepositioning MCMs to achieve better antibiotic efficacy. Prepositioning though also has drawbacks as we discussed before, for example, it increases cost due to higher inventory management and replenishment costs and the loss of pooling effect downstream. We now discuss how to calibrate our model to navigate the underlying tradeoffs. For the purposes of this study, we consider the (LLG) formulation, that is, policymakers specify coverage targets and our model calculates the minimum required inventory costs.

Model calibration. In our case study, we consider the prepositioning of one MCM type, *e.g.*, *ciprofloxacin* or *doxycycline*, to treat individuals affected by anthrax attacks in any of the 336 major metropolitan statistical areas (MSA) in the U.S. (according to Census Bureau [46]). There are twelve federally-managed SNS warehouses in the U.S. for MCM storage, with their exact locations being classified for security reasons. Instead, it is publicly known that the locations have been chosen such that MCMs can be transported from them to any U.S. state within 24-36 hours of a deployment decision [37]. Within our model, it is appropriate then to consider these warehouses as a single virtual federal stockpile node. In case of an attack, inventories can be shipped from the federal inventory node to state-managed warehouses, where additional inventory is usually stored. Inventory from these warehouses can then be forwarded to city and local authorities for dispensing to the general public. We therefore model the SNS stockpile network with 1 federal stockpile node, 52 state level stockpile nodes, and 336 MSA nodes.

As we remarked above, the time to ship MCMs from the federal node to any state level node varies between 24 to 36 hours. Within each state, we assume the transportation time to be within 2 to 6 hours, *e.g.*, if shipped via ground transportation, depending on the geography of the state. According to performed field studies, including, for example, a field study in Philadelphia in 2005 [1] and another one in Minneapolis in 2008 [4], policymakers have estimated the dispensing of MCMs from local authorities to individuals to take 10 to 12 hours, either via public dispensing facilities or postal/courier service. Using these figures, we can calculate the survivability parameters for each link in the network according to equation (16): $\rho_{ij} = \rho(\tau_0 + \tau_{ij})$, where τ_0 is the detection time and τ_{ij} is the time between shipment from stockpile i and dispensing at demand node j.

Inventory costs include the cost of purchasing, storage, management, replenishment, and shipment from manufacturer to warehouse. According to a commissioned paper by the Institute of

Medicine [19], the costs for anthrax antibiotics stored at regional warehouses amount to \$2.10 per person, while home kits are more expensive at \$10 per person, due to higher packaging and delivery costs. We estimate the federal and state stockpile costs to be \$1 and \$2 per person, due to anticipated scale economies. Annual management and replenishment costs are 85% of cost [19].

To estimate the demand volume at each MSA in case of an attack, we assume that an airborne attack has the same spread radius in every geographic region, and we use a value of 3,000 square miles as in the field study on the Minneapolis MSA [4]. The affected population at node i can then be calculated as (population density of i) $\times$ min{3000 sq miles, area of MSA}. We obtained population density and area data of MSAs from statistics of the Census Bureau [46].

Results. Having calibrated the model, we compute optimal inventory configurations and costs for different policy parameters: survivability target, attack scale, and detection time. Table 3 is a summary of the model inputs and outputs.

Input	**Output**
Survivability target: ϵ_i	Total inventory holding cost
Attack scale: Γ_i	Optimal inventory prepositioning strategy: $\mathbf{x}^\star$
Detection time: τ_0	

Table 3 Input/output for our case study.

The default input parameters we consider are survivability targets $1-\epsilon_i = 0.94$, $\forall i \in V_D$, attack scale parameters $\Gamma_i = 2$, $\forall i \in V$, and detection time $\tau_0 = 48$ hours.[5] Below, we perform several sensitivity analyses to illustrate the flexibility of our framework and how it can be used to guide policy making.

1. *Varying survivability target.* Figure 6 depicts the minimum required annual inventory cost as a function of the survivability target. For example, for a 90% survivability target the annual inventory budget needs to be about \$77 million annually; if the survavibility target is set to 95%, the budget would need to be increased to \$330 million, approximately. The curve in Figure 6 also illustrates that increasing the survivability target beyond 90% requires a rather steep cost increase. We can also interpret the curve as a Pareto frontier associated with the cost-survivability tradeoff: the region left to the curve represents the achievable outcomes.

   Figure 7 shows how much inventory and where it needs to be prepositioned for different survivability targets. We obsvere that for low targets, storing small amounts of inventory at the federal level, *i.e.*, level 0, is sufficient. As the target increases, more inventory is required, which is stored at the state (level 1) or MSA levels (level 2). Interestingly, predispensing medical kits (level 3) is not cost-efficient in any of these cases.

[5] For a discussion of anticipated detection times in case of an anthrax attack, see [43].

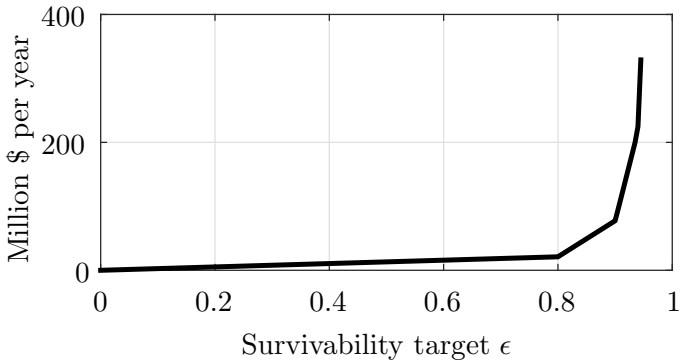

Figure 6 Minimum required annual inventory costs for different survivability targets.

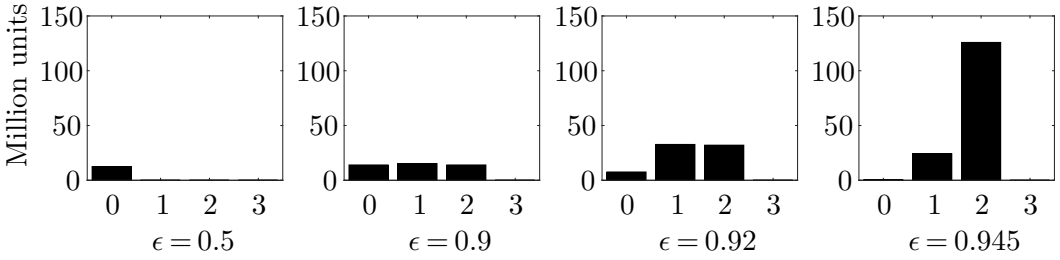

Figure 7 Amount (y-axis) and location (x-axis) of prepositioned inventory for different survivability targets $\{0.5, 0.9, 0.92, 0.945\}$; at the x-axis, level 0 is federal, level 1 is state, level 2 is MSA, and level 3 is predispensed medical kits in households.

	# Cities = 1	# Cities = 2	# Cities = 3
# States = 1	\$832 mil	\$1121 mil	\$1306 mil
# States = 2	\$835 mil	\$1124 mil	\$1310 mil
# States = 3	\$838 mil	\$1127 mil	\$1314 mil

Table 4 Minimum required annual costs for different attack scale parameters Γ_i.

2. *Varying attack scale.* We now explore different attack scale parameters. Table 4 and Figure 8 report the minimun required annual costs and optimal inventory amounts at each level, under nine different cases: $\{1, 2, 3\}$ states being attacked and each state having $\{1, 2, 3\}$ cities affected. Recall that the first parameter reflects the geographic complexity of the attack, and the second parameter the magnitude of an attack within a state. For this particular setup, the total cost is much more sensitive on the attack magnitude as compared with the attack complexity, since the policymaker already needs to preposition a large quantity of MCMs at the MSA level (level 2) in order to achieve the default survivability target of 0.94.
3. *Varying detection time.* Figure 9 shows the cost-survivability tradeoff for different detection times, highlighting the importance of timely response mechanisms. In particular, if detection infrastructure is able to detect an attack within 60 hours, approximately \$350 million of

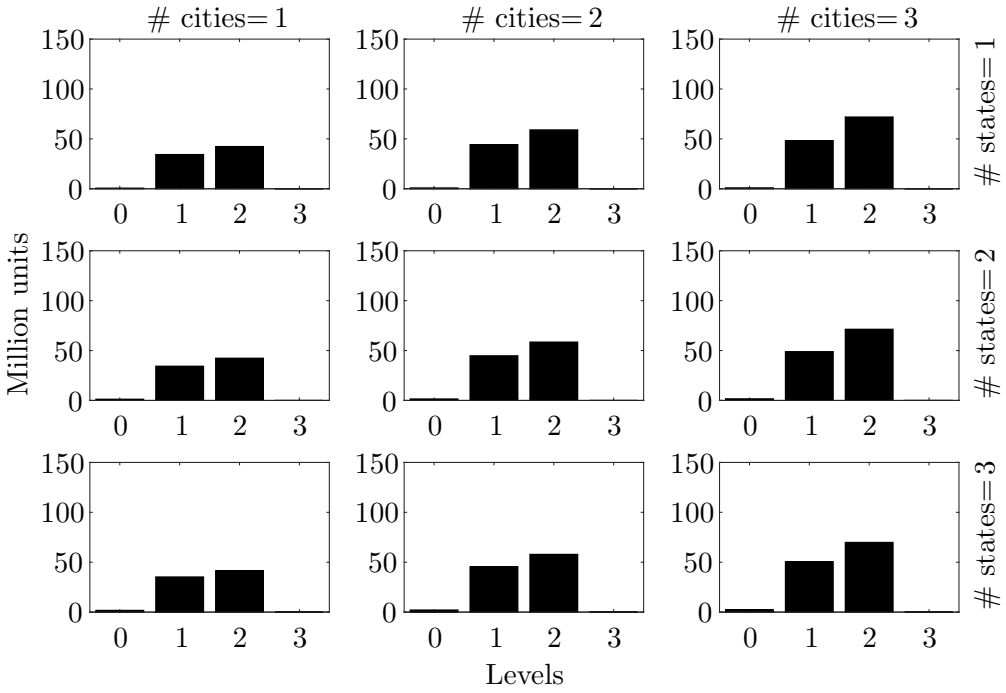

Figure 8 Amount (y-axis) and location (x-axis) of prepositioned inventory for different attack scale parameters; at the x-axis, level 0 is federal, level 1 is state, level 2 is MSA, and level 3 is predispensed medical kits in households.

annual inventory costs are needed for a 92.5% survivability target. For enhanced detection infrastructure capable of detecting attacks within 24 hours, the corresponding annual costs reduce to just over $23 million.

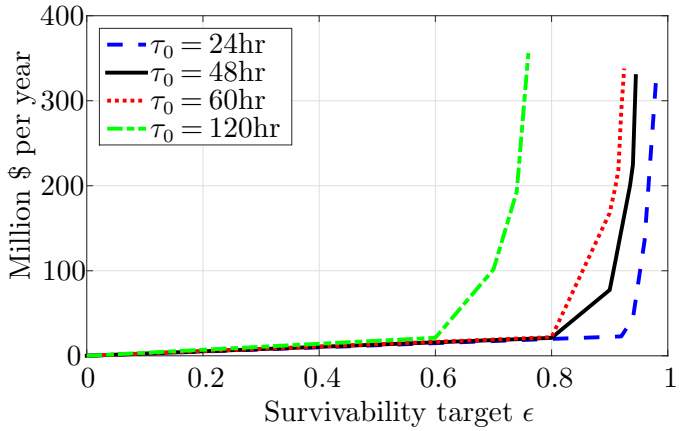

Figure 9 Minimum required annual inventory costs for different survivability targets and detection times.

6. Extensions and Concluding Remarks

In this paper, we presented a framework to tackle the problem of prepositioning MCM inventory to build a cost-effective and responsive public health stockpile network for protection against bioterrorism attacks. Our framework captured many of the key drivers facing the CDC in maintaining the Strategic National Stockpile, for example, holding costs, pooling, and responsiveness. Our methodology can be extended to capture additional SNS design considerations, or used in other supply chain applications.

Additional SNS design considerations. During bioattacks, the delivery of shipped MCMs to the public takes place at public dispensing facilities, called Point of Dispenses. CDC has identified that for certain cases, such as large-scale anthrax attacks, the POD dispensing capacity could become a bottleneck in some locations. In our model, we have so far assumed no dispensing capacity limitations. In particular, inventory shipped from node i to node j has the same efficacy (as measured via the survival probability ρ_{ij}), independent of the quantity. In the face of limited dispensing capacity, efficacy of incremental shipments could indeed decrease. An interesting research direction would be to extend our model to capture such capacity constraints. Moreover, it would be useful to consider a formulation that allows POD capacity design as well, in conjunction with inventory prepositioning decisions.

Another interesting direction for future research could be to allow for multiple types of MCMs, for the same or different biothreats. In that case, our model could be used to guide the design of the CDC's overall portfolio and mix of MCMs in view of budgetary constraints.

Application to Supply Chain Design and Comparison with Stochastic Optimization. The MCM inventory prepositioning problem we studied in this paper is essentially a two-stage inventory allocation and shipment problem in view of demand surges. Such a model can be applied to other domains of interest as well, for example, supply chain, manufacturing and distribution networks. In these contexts, managers usually face the problem of maintaining appropriate inventory safety stock levels across their networks to hedge against unforeseen disruptions to their usual course of operation. These stocking decisions need to be made in conjunction with contingent shipping policies, in a similar manner as in our model. Consequently, our model could be extended to tackle problems in these domains as well.

In the aforementioned contexts, however, disruption patterns are not neccessarily adversarial (as bioattacks are). A natural question to ask then is whether our robust optimization model would be suitable, as opposed to a stochastic optimization approach. In Appendix D, we demonstrate experimentally that if distributional information about the disruptions is imprecise, our robust optimization approach remains suitable. Readers are referred to the appendix for more details.

Acknowledgment

This work is supported by Ford Motor Company, The Boeing Company, and United Technologies Corporation.

References

[1] Mary Agócs, Shannon Fitzgerald, Steven Alles, Graham John Sale, Victor Spain, Edward Jasper, Thomas Lee Grace, and Esther Chernak. Field Testing a Head-of-Household Method to Dispense Antibiotics. *Biosecurity and Bioterrorism: Biodefense Strategy, Practice, and Science*, 5(3):255–267, sep 2007.

[2] Ravindra K Ahuja, Thomas L Magnanti, and James B Orlin. Network flows: theory, algorithms, and applications. *Prentice Hall*, 1993.

[3] Amir Ardestani-Jaafari and Erick Delage. Robust Optimization of Sums of Piecewise Linear Functions with Application to Inventory Problems. *Operations Research*, 64(2):474–494, apr 2016.

[4] Assistant Secretary for Preparedness and Response. National postal model for the delivery of medical countermeasures. Technical report, Department of Health and Human Services, Washington, D.C., 2010.

[5] Alper Atamtürk and Muhong Zhang. Two-Stage Robust Network Flow and Design Under Demand Uncertainty. *Operations Research*, 55(4):662–673, aug 2007.

[6] Aharon Ben-Tal, Laurent El Ghaoui, and Arkadi Nemirovski. Robust Optimization. *Princeton University Press*, 2009.

[7] Oded Berman and Arieh Gavious. Location of terror response facilities: A game between state and terrorist. *European Journal of Operational Research*, 177(2):1113–1133, mar 2007.

[8] Dimitris Bertsimas and Vineet Goyal. On the power and limitations of affine policies in two-stage adaptive optimization. *Mathematical Programming*, 134(2):491–531, sep 2012.

[9] Dimitris Bertsimas, Vineet Goyal, and Xu Andy Sun. A geometric characterization of the power of finite adaptability in multistage stochastic and adaptive optimization. *Mathematics of Operations Research*, 36(1):24–54, 2011.

[10] Dimitris Bertsimas, Dan A. Iancu, and Pablo A. Parrilo. Optimality of Affine Policies in Multistage Robust Optimization. *Mathematics of Operations Research*, 35(2):363–394, may 2010.

[11] Dena M. Bravata, Gregory S. Zaric, Jon-Erik C. Holty, Margaret L. Brandeau, Emilee R. Wilhelm, Kathryn M. McDonald, and Douglas K. Owens. Reducing Mortality from Anthrax Bioterrorism: Strategies for Stockpiling and Dispensing Medical and Pharmaceutical Supplies. *Biosecurity and Bioterrorism: Biodefense Strategy, Practice, and Science*, 4(3):244–262, sep 2006.

[12] Ron Brookmeyer. The statistical analysis of truncated data: application to the Sverdlovsk anthrax outbreak. *Biostatistics*, 2(2):233–247, jun 2001.

[13] Ron Brookmeyer, Elizabeth Johnson, and Sarah Barry. Modelling the incubation period of anthrax. *Statistics in Medicine*, 24(4):531–542, feb 2005.

[14] Aakil M. Caunhye, Xiaofeng Nie, and Shaligram Pokharel. Optimization models in emergency logistics: A literature review. *Socio-Economic Planning Sciences*, 46(1):4–13, mar 2012.

[15] Melih Çelik, Özlem Ergun, Ben Johnson, Pinar Keskinocak, Álvaro Lorca, Pelin Pekgün, and Julie Swann. Humanitarian Logistics. In *2012 TutORials in Operations Research*, pages 18–49. INFORMS, oct 2012.

[16] Soo-Haeng Cho. The optimal composition of influenza vaccines subject to random production yields. *Manufacturing & Service Operations Management*, 12(2):256–277, 2010.

[17] David L. Craft, Lawrence M. Wein, and Alexander H. Wilkins. Analyzing Bioterror Response Logistics: The Case of Anthrax. *Management Science*, 51(5):679–694, may 2005.

[18] Özlem Ergun, Gonca Karakus, Pinar Keskinocak, Julie Swann, and Monica Villarreal. Operations Research to Improve Disaster Supply Chain Management. In *Wiley Encyclopedia of Operations Research and Management Science*. John Wiley & Sons, Inc., Hoboken, NJ, USA, jan 2011.

[19] James Guyton, Robert Kadlec, Chandresh Harjivan, Shabana Farooqi, Sheana Cavitt, and Joseph Buccina. A Cost and Speed Analysis of Strategies for Prepositioning Antibiotics for Anthrax. *Commissioned paper by the Institute of Medicine*, 2011.

[20] Nathaniel Hupert, Wei Xiong, Kathleen King, Michelle Castorena, Caitlin Hawkins, Cindie Wu, and John A. Muckstadt. Uncertainty and Operational Considerations in Mass Prophylaxis Workforce Planning. *Disaster Medicine and Public Health Preparedness*, 3(S2):S121–S131, dec 2009.

[21] Dan A Iancu, Maxim Sviridenko, Mayank Sharma, and Maxim Sviridenko. Supermodularity and Affine Policies in Dynamic Robust Optimization. *Operations Research*, 61(4):941–956, aug 2013.

[22] Thomas Inglesby and Barbara Ellis. Division of Strategic National Stockpile (DSNS) Program Review: A Report from the Board of Scientific Counselors (BSC). Technical report, Center for Disease Control and Prevention, Atlanta, 2012.

[23] Institute of Medicine. The 2009 H1N1 influenza vaccination campaign: Summary of a workshop series. *National Academies Press*, 2010.

[24] Jocelyn Kaiser. Taking Stock of the Biodefense Boom. *Science*, 333(6047):1214–1214, sep 2011.

[25] Edward H. Kaplan, Christopher A. Patton, William P. FitzGerald, and Lawrence M. Wein. Detecting Bioterror Attacks by Screening Blood Donors: A Best-Case Analysis. *Emerging Infectious Diseases*, 9(8):909–914, aug 2003.

[26] Kathleen King. Logistical Models For Planning And Operating Medical Countermeasure Distribution Networks During Public Health Emergencies. *PhD dissertation, Cornell University*, 2012.

[27] Kathleen King and John A. Muckstadt. Evaluating Planned Capacities for Public Health Emergency Supply Chain Models. Technical report, Cornell University, 2009.

[28] Eva K. Lee, Chien-Hung Chen, Ferdinand Pietz, and Bernard Benecke. Modeling and Optimizing the Public-Health Infrastructure for Emergency Response. *Interfaces*, 39(5):476–490, oct 2009.

[29] Eva K. Lee, Siddhartha Maheshwary, Jacquelyn Mason, and William Glisson. Decision support system for mass dispensing of medications for infectious disease outbreaks and bioterrorist attacks. *Annals of Operations Research*, 148(1):25–53, nov 2006.

[30] Eva K. Lee, Siddhartha Maheshwary, Jacquelyn Mason, and William Glisson. Large-Scale Dispensing for Emergency Response to Bioterrorism and Infectious-Disease Outbreak. *Interfaces*, 36(6):591–607, dec 2006.

[31] Eva K. Lee, Hannah K. Smalley, Yang Zhang, Ferdinand Pietz, and Bernard Benecke. Facility location and multi-modality mass dispensing strategies and emergency response for biodefence and infectious disease outbreaks. *International Journal of Risk Assessment and Management*, 12(2/3/4):311, 2009.

[32] Eva K Lee, Fan Yuan, Ferdinand H Pietz, Bernard A Benecke, and Greg Burel. Vaccine prioritization for effective pandemic response. *Interfaces*, 45(5):425–443, 2015.

[33] Helder I Nakaya, Jens Wrammert, Eva K Lee, Luigi Racioppi, Stephanie Marie-Kunze, W Nicholas Haining, Anthony R Means, Sudhir P Kasturi, Nooruddin Khan, Gui-Mei Li, Megan McCausland, Vibhu Kanchan, Kenneth E Kokko, Shuzhao Li, Rivka Elbein, Aneesh K Mehta, Alan Aderem, Kanta Subbarao, Rafi Ahmed, and Bali Pulendran. Systems biology of vaccination for seasonal influenza in humans. *Nature Immunology*, 12(8):786–795, jul 2011.

[34] Anna Nicholson, Scott Wollek, Benjamin Kahn, and Jack Hermann. The Nation's Medical Countermeasure Stockpile. *National Academies Press*, 2016.

[35] Office of Public Health Preparedness and Response. Board of Scientific Counselors, 2016.

[36] Office of Public Health Preparedness and Response. Public Health Preparedness Capabilities: National Standards for State and Local Planning, 2016.

[37] Office of Public Health Preparedness and Response. Strategic National Stockpile, 2016.

[38] Osman Y Özaltin, Oleg A Prokopyev, Andrew J Schaefer, and Mark S Roberts. Optimizing the societal benefits of the annual influenza vaccine: A stochastic programming approach. *Operations research*, 59(5):1131–1143, 2011.

[39] David Simchi-Levi, William Schmidt, and Yehua Wei. From superstorms to factory fires: managing unpredictable supply-chain disruptions. *Harvard Business Review*, 92(1-2):96, 2014.

[40] David Simchi-Levi, William Schmidt, Yehua Wei, Peter Yun Zhang, Keith Combs, Yao Ge, Oleg Gusikhin, Michael Sanders, and Don Zhang. Identifying Risks and Mitigating Disruptions in the Automotive Supply Chain. *Interfaces*, 45(5):375–390, oct 2015.

[41] David Simchi-Levi, He Wang, and Yehua Wei. Increasing Supply Chain Robustness through Process Flexibility and Inventory. *Working paper, MIT*, 2016.

[42] Hannah K Smalley, Pinar Keskinocak, Faramroze G Engineer, and Larry K Pickering. Universal tool for vaccine scheduling: applications for children and adults. *Interfaces*, 41(5):436–454, 2011.

[43] Clare Stroud, Kristin Viswanathan, Tia Powell, and Robert R Bass. Prepositioning Antibiotics for Anthrax. *Institute of Medicine*, (September):1–387, 2011.

[44] Anna Teytelman and Richard C Larson. Multiregional dynamic vaccine allocation during an influenza epidemic. *Service Science*, 5(3):197–215, 2013.

[45] Joline Uichanco. A robust model for pre-positioning emergency relief items before a typhoon with an uncertain trajectory. *Working paper, University of Michigan*, 2015.

[46] United States Census Bureau. Population, Housing Units, Area, and Density: 2000, 2000.

[47] L. M. Wein, D. L. Craft, and E. H. Kaplan. Emergency response to an anthrax attack. *Proceedings of the National Academy of Sciences*, 100(7):4346–4351, apr 2003.

[48] D. A. Wilkening. Sverdlovsk revisited: Modeling human inhalation anthrax. *Proceedings of the National Academy of Sciences*, 103(20):7589–7594, may 2006.

[49] D. A. Wilkening. Modeling the Incubation Period of Inhalational Anthrax. *Medical Decision Making*, 28(4):593–605, jul 2008.

[50] Joseph T Wu, Lawrence M Wein, and Alan S Perelson. Optimization of influenza vaccine selection. *Operations Research*, 53(3):456–476, 2005.

Appendix A: Proof of Proposition 1

Note that we can express $\Omega_i^F(\xi_i', x_i, \mathbf{x}_{-i})$ as $\max_{\boldsymbol{\xi}\in\Xi_i(\xi_i')} r_i(\boldsymbol{\xi}, x_i, \mathbf{x}_{-i})$, where

$$\begin{aligned} r_i(\boldsymbol{\xi}, x_i, \mathbf{x}_{-i}) := \min_{\mathbf{y},\mathbf{s}} \quad & \sum_{k\in V_i} s_k \\ \text{subject to} \quad & x_i \geq \sum_{j\in\mathcal{C}(i)} y_{ij} \\ & s_i + x_i \geq \sum_{j\in\mathcal{C}(i)} y_{ij} + \bar{d}_i + \hat{d}_i\xi_i \\ & y_{\mathcal{P}(k)k} + x_k \geq \sum_{j\in\mathcal{C}(k)} y_{kj},\ \forall k \in V_i\setminus\{i\} \\ & y_{\mathcal{P}(k)k} + s_k + x_k \geq \sum_{j\in\mathcal{C}(k)} y_{kj} + \bar{d}_k + \hat{d}_k\xi_k,\ \forall k \in V_i\setminus\{i\} \\ & \mathbf{y}, \mathbf{s} \geq 0. \end{aligned}$$

It is straightforward to check that the above optimization problem admits an optimal solution such that $s_i = (\bar{d}_i + \hat{d}_i\xi_i' - x_i)^+$ and $\sum_{j\in\mathcal{C}(i)} y_{ij} = (x_i - \bar{d}_i - \hat{d}_i\xi_i')^+$. Also,

$$r_i(\boldsymbol{\xi}, x_i + \Delta, \mathbf{x}_{-i}) = (r_i(\boldsymbol{\xi}, x_i, \mathbf{x}_{-i}) - \Delta)^+, \quad \forall \Delta \geq 0. \tag{18}$$

Another fact we will use is that

$$\min_{\substack{\mathbf{x}\geq 0 \\ \mathbf{1}'\mathbf{x}=K}} \sum_{i=1}^n (q_i - x_i)^+ = (\mathbf{1}'\mathbf{q} - K)^+, \quad \forall \mathbf{q}\in\mathbb{R}^n, K \geq 0. \tag{19}$$

Using all these properties we have

$$\Omega_i^F(\xi_i', x_i, \mathbf{x}_{-i}) = (\bar{d}_i + \hat{d}_i\xi_i' - x_i)^+ + \max_{\boldsymbol{\xi}\in\Xi_i} \min_{\substack{\{y_{ij}\}_{j\in\mathcal{C}(i)}: y_{ij}\geq 0, \\ \sum_{j\in\mathcal{C}(i)} y_{ij} = (x_i - \bar{d}_i - \hat{d}_i\xi_i')^+}} \sum_{j\in\mathcal{C}(i)} r_j(\boldsymbol{\xi}, x_j + y_{ij}, \mathbf{x}_{-j}) \tag{20a}$$

$$= (\bar{d}_i + \hat{d}_i\xi_i' - x_i)^+ + \max_{\boldsymbol{\xi}\in\Xi_i} \min_{\substack{\{y_{ij}\}_{j\in\mathcal{C}(i)}: y_{ij}\geq 0, \\ \sum_{j\in\mathcal{C}(i)} y_{ij} = (x_i - \bar{d}_i - \hat{d}_i\xi_i')^+}} \sum_{j\in\mathcal{C}(i)} (r_j(\boldsymbol{\xi}, x_j, \mathbf{x}_{-j}) - y_{ij})^+ \tag{20b}$$

$$= (\bar{d}_i + \hat{d}_i\xi_i' - x_i)^+ + \left(\max_{\boldsymbol{\xi}\in\Xi_i} \sum_{j\in\mathcal{C}(i)} r_j(\boldsymbol{\xi}, x_j, \mathbf{x}_{-j}) - (x_i - \bar{d}_i - \hat{d}_i\xi_i')^+ \right)^+ \tag{20c}$$

$$= (\bar{d}_i + \hat{d}_i\xi_i' - x_i)^+ + \left(\max_{\boldsymbol{\xi}_{\mathcal{C}(i)}\in \mathrm{proj}_{\mathcal{C}(i)}\Xi_i} \max_{\substack{\boldsymbol{\xi}\in\Xi_j(\xi_j), \\ j\in\mathcal{C}(i)}} \sum_{j\in\mathcal{C}(i)} r_j(\boldsymbol{\xi}, x_j, \mathbf{x}_{-j}) - (x_i - \bar{d}_i - \hat{d}_i\xi_i')^+ \right)^+ \tag{20d}$$

$$= (\bar{d}_i + \hat{d}_i\xi_i' - x_i)^+ + \left(\max_{\boldsymbol{\xi}_{\mathcal{C}(i)}\in \mathrm{proj}_{\mathcal{C}(i)}\Xi_i} \sum_{j\in\mathcal{C}(i)} \max_{\boldsymbol{\xi}\in\Xi_j(\xi_j)} r_j(\boldsymbol{\xi}, x_j, \mathbf{x}_{-j}) - (x_i - \bar{d}_i - \hat{d}_i\xi_i')^+ \right)^+ \tag{20e}$$

$$=(\bar{d}_i+\hat{d}_i\xi_i'-x_i)^+ + \left(\max_{\boldsymbol{\xi}_{\mathcal{C}(i)}\in \mathrm{proj}_{\mathcal{C}(i)}\Xi_i} \sum_{j\in\mathcal{C}(i)} \Omega_j^F(\xi_j,x_j,\mathbf{x}_{-j}) - (x_i-\bar{d}_i-\hat{d}_i\xi_i')^+\right)^+ \tag{20f}$$

$$=\left(\bar{d}_i+\hat{d}_i\xi_i'-x_i+\max_{\boldsymbol{\xi}_{\mathcal{C}(i)}\in \mathrm{proj}_{\mathcal{C}(i)}\Xi_i} \sum_{j\in\mathcal{C}(i)} \Omega_j^F(\xi_j,x_j,\mathbf{x}_{-j})\right)^+. \tag{20g}$$

Equality (20a) follows from the definition of r_i; (20b) follows from (18); (20c) follows from (19); (20d) is an equivalent way of writing the maximization operator; exchanging the inner maximization and summation operators is allowed since r_j only depends on $\{\xi_k, k\in V_j\}$, leading to (20e); (20f) follows from the definition of r_j. Equality (20g) holds by considering the fact that $\Omega_j^F\geq 0$ for any $j\in\mathcal{C}(i)$, and checking two cases: one with $\bar{d}_i+\hat{d}_i\xi_i'-x_i<0$, and the other with $\bar{d}_i+\hat{d}_i\xi_i'-x_i\geq 0$.

To show convexity of $\Omega_i^F(\xi_i',x_i,\mathbf{x}_{-i})$, we use an induction argument on the level of node i. First note that for $i\in V^L$, we have $\Omega_i^F(\xi_i',x_i,\mathbf{x}_{-i})=(\bar{d}_i+\hat{d}_i\xi_i'-x_i)^+$, which is convex and non-decreasing in ξ_i'. For i in any other level of the network, given the result we just proved (20g), it suffices to show $\max_{\boldsymbol{\xi}_{\mathcal{C}(i)}\in \mathrm{proj}_{\mathcal{C}(i)}\Xi_i(\xi_i')} \sum_{j\in\mathcal{C}(i)} \Omega_j^F(\xi_j,x_j,\mathbf{x}_{-j})$ is convex in ξ_i'. Since $\Omega_j^F(\xi_j,x_j,\mathbf{x}_{-j})$ is convex in ξ_j (by the induction hypothesis), maximum is obtained at the extreme points. Given that $\mathrm{proj}_{\mathcal{C}(i)}\Xi_i(\xi_i')=\{\boldsymbol{\xi}_{\mathcal{C}(i)}:\xi_j\in[0,\xi_i'],\mathbf{1}'\boldsymbol{\xi}_{\mathcal{C}(i)}\leq\Gamma_i\xi_i'\}$ and Ω_j^F is non-decreasing in ξ_j, we can equivalently write: $\max_{|S|=\Gamma_i,S\subseteq\mathcal{C}(i)}\left\{\sum_{j\in S}\Omega_j^F(\xi_i',x_j,\mathbf{x}_{-j})+\sum_{j\in\mathcal{C}(i)\setminus S}\Omega_j^F(0,x_j,\mathbf{x}_{-j})\right\}$, which is convex and non-decreasing in ξ_i'. □

Appendix B: Proof of Proposition 2

For the sake of reaching a contradiction, suppose there exists some extreme point $\boldsymbol{\xi}\in\mathrm{ext}(\Xi)$, such that its kth entry is fractional, $\xi_k\in(0,1)$. Note that by definition of Ξ, $\xi_0=1$, and thus $k\neq 0$. Let $p=\mathcal{P}(k)$ be its parent, *i.e.*, $k\in\mathcal{C}(p)$. Then it must hold that $0<\sum_{i\in\mathcal{C}(p)}\xi_i\leq\Gamma_p\xi_p$, and thus $\Gamma_p>0$ and $\xi_p>0$.

Suppose $\xi_p=1$. Then the above condition becomes $0<\sum_{i\in\mathcal{C}(p)}\xi_i\leq\Gamma_p$. Furthermore, $\xi_i\in[0,1]$ $\forall i\in\mathcal{C}(p)$. Now consider the $|\mathcal{C}(p)|$-dimensional polytope $\{\boldsymbol{\gamma}:\sum_{i\in\mathcal{C}(p)}\gamma_i\leq\Gamma_p,\gamma_i\in[0,1]\,\forall i\in\mathcal{C}(p)\}$, which can be readily seen to have binary extreme points. Let these extreme points be $\{\boldsymbol{\gamma}^j,j=1,\ldots,N\}$. Since $\boldsymbol{\xi}_{\mathcal{C}(p)}$ belongs to this polytope, we can express it as

$$\boldsymbol{\xi}_{\mathcal{C}(p)}=\sum_{j=1}^N\alpha_j\boldsymbol{\gamma}^j,\ \text{where}\ \sum_{j=1}^N\alpha_j=1,\alpha_j\geq 0,\forall j\in\{1,\ldots,N\}.$$

In particular, for those $i\in\mathcal{C}(p)$ that $\xi_i>0$, we have:

$$\sum_{j=1}^N\alpha_j\gamma_i^j=\xi_i\iff\sum_{j=1}^N\alpha_j\frac{1}{\xi_i}\gamma_i^j=1. \tag{21}$$

Now we use each $\boldsymbol{\gamma}^j$ to construct a vector $\boldsymbol{\xi}^j\in\Xi$ and show that we can write $\boldsymbol{\xi}$ as a convex combination of $\{\boldsymbol{\xi}^j,j=1,\ldots,N\}$, and $\boldsymbol{\xi}\neq\boldsymbol{\xi}^j,\forall j\in\{1,\ldots,N\}$—which will contradict our assumptions.

We construct $\boldsymbol{\xi}^j$, $j=1,\ldots,N$, as follows:

$$\begin{aligned}
\boldsymbol{\xi}^j_{V\setminus V_p} &= \boldsymbol{\xi}_{V\setminus V_p},\\
\xi^j_p &= \xi_p,\\
\boldsymbol{\xi}^j_{\mathcal{C}(p)} &= \boldsymbol{\gamma}^j,\\
\boldsymbol{\xi}^j_{V_i\setminus\{i\}} &= \begin{cases} \frac{1}{\xi_i}\boldsymbol{\xi}_{V_i\setminus\{i\}} & \text{if } \xi_i>0 \text{ and } \xi^j_i=1\\ 0 & \text{otherwise}\end{cases}, \quad \forall i\in\mathcal{C}(p).
\end{aligned}$$

It is straightforward to verify that for all $j=1,\ldots,N$, $\boldsymbol{\xi}^j\in\Xi$ and $\boldsymbol{\xi}^j\neq\boldsymbol{\xi}$. We next argue that $\sum_{j=1,\ldots,N}\alpha_j\boldsymbol{\xi}^j=\boldsymbol{\xi}$ by checking component-wise. This is straightforward for components $V\setminus V_p$, p, and $\mathcal{C}(p)$. For any $l\in V_i\setminus\{i\}$ for $i\in\mathcal{C}(p)$ such that $\xi_i=0$, we have that $\xi^j_l=\xi_l=0$ for all $j=1,\ldots,N$. Finally, for any $l\in V_i\setminus\{i\}$ for $i\in\mathcal{C}(p)$ such that $\xi_i>0$, we have that

$$\sum_{j=1}^N\alpha_j\xi^j_l=\sum_{j:\xi^j_i=1}\alpha_j\xi_l/\xi_i+\sum_{j:\xi^j_i=0}0=\sum_{j=1}^N\alpha_j\xi_l/\xi_i\xi^j_i=\sum_{j=1}^N\left(\alpha_j\xi^j_i/\xi_i\right)\xi_l=\sum_{j=1}^N\left(\alpha_j\gamma^j_i/\xi_i\right)\xi_l\overset{(21)}{=}\xi_l.$$

Consequently, $\boldsymbol{\xi}$ cannot be an extreme point if $\xi_p=1$. Since $\xi_p>0$, we must have $\xi_p\in(0,1)$. We can propagate this argument upstream to eventually show that $\xi_0\in(0,1)$, which contradicts that $\xi_0=1$ for all $\boldsymbol{\xi}\in\Xi$, and the proof is complete. $\square$

Appendix C: Proof of Proposition 3

We proceed by checking two cases: $\alpha_i<1$ and $\alpha_i=1$.

Case $\alpha_i<1$:

Let $\{\bar{\mathbf{y}}^{j1},\bar{\mathbf{s}}^{j1}\}\in\overline{\mathcal{Q}}^*_{j1}$. Define $\{\bar{\mathbf{y}}^{j0},\bar{\mathbf{s}}^{j0}\}$ such that $\bar{\mathbf{y}}^{j0}(0)=\bar{\mathbf{y}}^{j1}(0)$, $\bar{s}^{j0}_k(0)=\bar{s}^{j1}_k(0)\ \forall k\in V_j\setminus\{j\}$, $\bar{s}^{j0}_j(0)=(\sum_{k\in\mathcal{C}(j)}\bar{y}^{j0}_{jk}(0)+\bar{d}_i-x_j-\alpha_i g^0_j)^+$. We will show that $\{\bar{\mathbf{y}}^{j0},\bar{\mathbf{s}}^{j0}\}\in\overline{\mathcal{Q}}^\star_{j0}$, thus showing the result.

For (I), because $\Xi_j(0)$ contains only a single value 0, there is nothing to check.

For (II), if the if-condition holds at node j, then $\bar{y}^{j0}_{jk}(0)=\bar{y}^{j1}_{jk}(0)=\Omega^A_k(0,x_k,\mathbf{x}_{-k})\forall k\in\mathcal{C}(j)$ and $x_j+\alpha_i g^0_j\geq\bar{d}_j+\sum_{k\in\mathcal{C}(j)}\Omega^A_k(0,x_k,\mathbf{x}_{-k})=\bar{d}_j+\sum_{k\in\mathcal{C}(j)}\bar{y}^{j1}_{jk}(0)\implies\bar{s}^{j0}_j(0)=0$; (IIa) and (IIb) hold for other nodes by construction. If the if-condition holds for any node other than j, (II) holds for $\{\bar{\mathbf{y}}^{j0},\bar{\mathbf{s}}^{j0}\}$ since (II) holds for $\{\bar{\mathbf{y}}^{j1},\bar{\mathbf{s}}^{j1}\}$.

For (III), (IIIa) does not need to be checked since $\Xi_j(0)$ contains only 0, and (IIIc) holds by construction. For (IIIb), if $\bar{s}^{j0}_j(0)=(\sum_{k\in\mathcal{C}(j)}\bar{y}^{j0}_{jk}(0)+\bar{d}_i-x_j-\alpha_i g^0_j)^+>0$, then $\bar{s}^{j0}_j(0)=\sum_{k\in\mathcal{C}(j)}\bar{y}^{j0}_{jk}(0)+\bar{d}_i-x_j-\alpha_i g^0_j\implies\bar{s}^{j0}_j(0)+x_j+\alpha_i g^0_j=\sum_{k\in\mathcal{C}(j)}\bar{y}^{j0}_{jk}(0)+\bar{d}_i$. If $\exists k\in V_j\setminus\{j\}$ such that $\bar{s}^{j1}_k(0)>0$, then the equality of (IIIb) holds for all nodes $V^+_j(\bar{\mathbf{s}}^{j0})\setminus\{j\}$. For node j, we have $x_j+\alpha_i g^0_j+\bar{s}^{j1}_j(1)=\sum_{k\in\mathcal{C}(j)}\bar{y}^{j1}_{jk}(1)+\bar{d}_j+\hat{d}_j\overset{\text{IIIa}}{\implies}x_j+\alpha_i g^0_j+\bar{s}^{j1}_j(1)=\sum_{k\in\mathcal{C}(j)}\bar{y}^{j1}_{jk}(0)+\bar{d}_j+\hat{d}_j\implies x_j+\alpha_i g^0_j+\bar{s}^{j1}_j(1)=\sum_{k\in\mathcal{C}(j)}\bar{y}^{j0}_{jk}(0)+\bar{d}_j+\hat{d}_j$. But since $\bar{s}^{j1}_j(1)\geq\hat{d}_j$, we have $x_j+\alpha_i g^0_j\leq\sum_{k\in\mathcal{C}(j)}\bar{y}^{j0}_{jk}(0)+\bar{d}_j$, then by the definition of $\bar{s}^{j0}_j(0)$, $x_j+\alpha_i g^0_j+\bar{s}^{j0}_j(0)=\sum_{k\in\mathcal{C}(j)}\bar{y}^{j0}_{jk}(0)+\bar{d}_j$. (IIIc) holds by definition.

To show constraint satisfaction, *i.e.*, $\{\bar{\mathbf{y}}^{j0}, \bar{\mathbf{s}}^{j0}\} \in \mathcal{Q}_j(0, x_j, \mathbf{x}_{-j})$, we know that all constraints that do not involve $\bar{s}_j^{j0}(0)$ are satisfied by the feasibility of $\{\bar{\mathbf{y}}^{j1}, \bar{\mathbf{s}}^{j1}\}$. Constraints involving $\bar{s}_j^{j0}(0)$, *i.e.*, $\bar{s}_j^{j0}(0) + x_j + \alpha_i g_j^0 \geq \sum_{k\in\mathcal{C}(j)} \bar{y}_{jk}^{j0}(0) + \bar{d}_j$ and $\bar{s}_j^{j0}(0) \geq 0$, are satisfied by the definition of $\bar{s}_j^{j0}(0)$.

To show optimality of $\{\bar{\mathbf{y}}^{j0}, \bar{\mathbf{s}}^{j0}\}$, since it satisfies (III), this holds for all $k \in V_j^+(\bar{\mathbf{s}}^{j0})$: $\bar{y}_{\mathcal{P}(k)k}^{j0}(0) + x_k + \alpha_i g_j^0 \mathbb{1}_{k=j} + \bar{s}_k^{j0}(0) = \sum_{m\in\mathcal{C}(k)} \bar{y}_{km}^{j0}(0) + \bar{d}_k$. Let $V_j^\star(\bar{\mathbf{s}}^{j0}) := \{m \in V \setminus V_j^+(\bar{\mathbf{s}}^{j0}) : \exists k \in V_j^+(\bar{\mathbf{s}}^{j0}) \text{ s.t. } m \in \mathcal{C}(k), \Omega_m^A(0, x_m, \mathbf{x}_{-m}) > 0\}$.

Thus (using shorthand V^+ for $V_j^+(\bar{\mathbf{s}}^{j0})$ and $V^\star$ for $V_j^\star(\bar{\mathbf{s}}^{j0})$),

$$
\begin{aligned}
&\sum_{k\in V^+} \bar{y}_{\mathcal{P}(k)k}^{j0}(0) + \sum_{k\in V^+} x_k + \alpha_i g_j^0 + \sum_{k\in V^+} \bar{s}_k^{j0}(0) = \sum_{k\in V^+} \sum_{m\in\mathcal{C}(k)} \bar{y}_{km}^{j0}(0) + \sum_{k\in V^+} \bar{d}_k \\
\overset{\text{(IIa)}}{\Longrightarrow} &\sum_{k\in V^+} \bar{y}_{\mathcal{P}(k)k}^{j0}(0) + \sum_{k\in V^+} x_k + \alpha_i g_j^0 + \sum_{k\in V^+} \bar{s}_k^{j0}(0) = \sum_{k\in V^+} \bar{y}_{\mathcal{P}(k)k}^{j0}(0) + \sum_{k\in V^\star} \bar{y}_{\mathcal{P}(k)k}^{j0}(0) + \sum_{k\in V^+} \bar{d}_k \\
\Longrightarrow &\sum_{k\in V^+} \bar{s}_k^{j0}(0) = \sum_{k\in V^+} \bar{d}_k - \sum_{k\in V^+} x_j - \alpha_i g_j^0 + \sum_{k\in V^\star} \bar{y}_{\mathcal{P}(k)k}^{j0}(0) \\
\Longrightarrow &\sum_{k\in V^+} \bar{s}_k^{j0}(0) = \sum_{k\in V^+} \bar{d}_k - \sum_{k\in V^+} x_j - \alpha_i g_j^0 + \sum_{k\in V^\star} \Omega_k^A(0, x_k, \mathbf{x}_{-k}) \qquad \text{(optimality of } \bar{\mathbf{y}}^{j1}) \\
\Longrightarrow &\sum_{k\in V_j} \bar{s}_k^{j0}(0) = \sum_{k\in V^+} \bar{d}_k - \sum_{k\in V^+} x_k - \alpha_i g_j^0 + \sum_{k\in V^\star} \Omega_k^A(0, x_k, \mathbf{x}_{-k}).
\end{aligned}
$$

Since $V \setminus \{\cup_{k\in V^\star} V_k \cup V^+\}$ is downstream from the nodes in $\cup_{k\in V^\star} V_k \cup V^+$, the total demand loss in V_j, $\Omega_j^A(0, x_j, \mathbf{x}_{-j})$, is no less than the demand loss in the subset of nodes $\cup_{k\in V^\star} V_k \cup V^+$, which is in turn lowerbounded by $\sum_{k\in V^\star} \Omega_k^A(0, x_k, \mathbf{x}_{-k}) + \sum_{k\in V^+} \bar{d}_k - \sum_{k\in V^+} x_k - \alpha_i g_j^0$. Therefore, $\{\bar{\mathbf{y}}^{j0}, \bar{\mathbf{s}}^{j0}\}$ achieves the optimal cost, $\{\bar{\mathbf{y}}^{j0}, \bar{\mathbf{s}}^{j0}\} \in \overline{\mathcal{Q}}_{j0}^\star$.

Case $\alpha_i = 1$:

By the definition of α_i, we have $x_i \geq \bar{d}_i + \sum_{j\in\mathcal{C}(i)} \Omega_j^A(0, x_j, \mathbf{x}_{-j})$. Since $\{\bar{\mathbf{y}}^{j0}, \bar{\mathbf{s}}^{j0}\}$ and $\{\bar{\mathbf{y}}^{j1}, \bar{\mathbf{s}}^{j1}\}$ satisfy (II), $\bar{y}_{km}^{j0}(0) = \bar{y}_{km}^{j1}(0) = \Omega_m^A(0, x_m, \mathbf{x}_{-m})$ for $(k, m) \in T_j, j \in \mathcal{C}(i)$, thus $\bar{\mathbf{y}}^{j0} = \bar{\mathbf{y}}^{j1}$. Also, $\bar{s}_k^{j0}(0) = 0$ and $\bar{s}_k^{j1}(0) = 0 \; \forall k \in V_j \setminus \{j\}$, so $\bar{s}_k^{j0}(0) = \bar{s}_k^{j1}(0) \; \forall k \in V_j \setminus \{j\}, j \in \mathcal{C}(i)$, this concludes the proof. □

Appendix D: Comparison with Stochastic Optimization

We compare our robust optimization solution approach with sample average approximation (SAA), which is a classical stochastic optimization solution approach. For a fair comparison, we will use mis-specified distributional information to calibrate both solution methods. We find that as mis-specification becomes more acute, our method outperforms SAA. We next describe the experimental setup in detail.

We use the same network structure as in Section 4.2. An uncertain scenario is chosen as follows. First, nature decides the number of level 1 nodes to impact, which we denote by γ. This random variable is described by a discrete Weibull distribution normalized on $\gamma = 1, \ldots, 4$, parameterized by (p, β): $\mathbb{P}[\gamma = x] = \frac{(1-p)^{x^\beta} - (1-p)^{(x+1)^\beta}}{(1-p) - (1-p)^{5^\beta}}$. Then, nature decides which level 1 nodes to affect: the

probability of picking i on the first run is increasing in the average demand of the node i. In this experiment, we let it be $p_i = \frac{\sum_{j\in\mathcal{C}(i)} p_j}{\sum_{j\in V_D} p_j}$, and we will define p_j shortly for the level 2 nodes. If there is any remaining budget, nature will move on to pick the next target with the probability proportional to its corresponding $p_i = \sum_{j\in\mathcal{C}(i)} p_j$. For each level 1 node picked, we assume that nature only picks one level 2 node. The probability of picking such node is proportional to p_j, which is increasing in the average demand, which we denote by μ_i: $p_i = \frac{\mu_i^2}{\sum_{i\in V_D}\mu_i^2}$. Finally, when a level 2 node sees high demand, the exact demand magnitude is characterized by a normal distribution with mean and standard deviation (μ_i, σ_i).

The SAA solution approach is based on the following formulation:

$$
\begin{aligned}
\min_{\mathbf{x},\mathbf{f},\mathbf{s}} \quad & \mathbf{h}'\mathbf{x} + \frac{1}{N}\sum_{k=1}^{N}[\mathbf{1}'\mathbf{s}^k(\mathbf{d}^k) + \mathbf{c}'\mathbf{f}^k(\mathbf{d}^k)] \\
\text{subject to} \quad & s_i^k(\mathbf{d}^k) + \sum_{j:(j,i)\in E} f_{ji}^k(\mathbf{d}^k) + x_i \geq \sum_{j:(i,j)\in E} f_{ij}^k(\mathbf{d}^k) + d_i^k, \quad \forall i\in V,\, k=1,\ldots,N \\
& \sum_{j:(j,i)\in E} f_{ji}^k(\mathbf{d}^k) + x_i \geq \sum_{j:(i,j)\in E} f_{ij}^k(\mathbf{d}^k), \quad \forall i\in V,\, k=1,\ldots,N \\
& \mathbf{x}, \mathbf{f}^k, \mathbf{s}^k \geq \mathbf{0}, \quad k=1,\ldots,N.
\end{aligned}
$$

The samples used are based on a presumed distribution (parameterized by (p^f, β^f) and $\{\mu_i^f, \sigma_i^f\}_i$). We then evaluate the solution by computing the cost under a potentially different actual distribution, parameterized by (p^a, β^a) and $\{\mu_i^a, \sigma_i^a\}_i$. The demand for node i, μ_i^a, is uniformly distributed between $[0.5, 1.5]\times\mu_i^f$, and the standard deviation is scaled accordingly. We consider twelve different forecast probability distributions, parameterized by $\beta^f \in \{1,2,3,4\}$ and $p^f \in \{0.3, 0.6, 0.9\}$. We then evaluate the SAA optimal solution against these twelve probability distributions.

We then use our robust optimization model, as follows. We construct the uncertainty set by letting the attack scale $\Gamma_i = 2$ for the level 1 nodes, and demand shock $\hat{d}_j = \mu_i + z\sigma_i$. We test with $z\in\{1,2,3\}$ and present the results for $z=2$ (the other two are not qualitatively different).

Figure 10 reports the obtained costs under both approaches. We observe that the robust solutions are less susceptible to probability distribution mis-specifications, unlike the stochastic optimization solutions, which are more volatile. A closer look at the cost breakdown reveals that the volatility is due entirely to the demand loss penalty.

	Stochastic		*Robust*		*Num. of Instances*
	mean	cv (%)	mean	cv (%)	
Exact	8,852	50	10,007	42	12
Close	9,507	49	10,117	35	86
Far	14,493	65	11,371	36	46
Overall	11,045	63	10,508	37	144

Table 5 Mean and coefficient of variation for different instances. "Exact": forecast and actual demand distributions are identical; "close": absolute difference in β is less than or equal to 2, and the absolute difference in p is less than or equal to 0.3; "far": the rest.

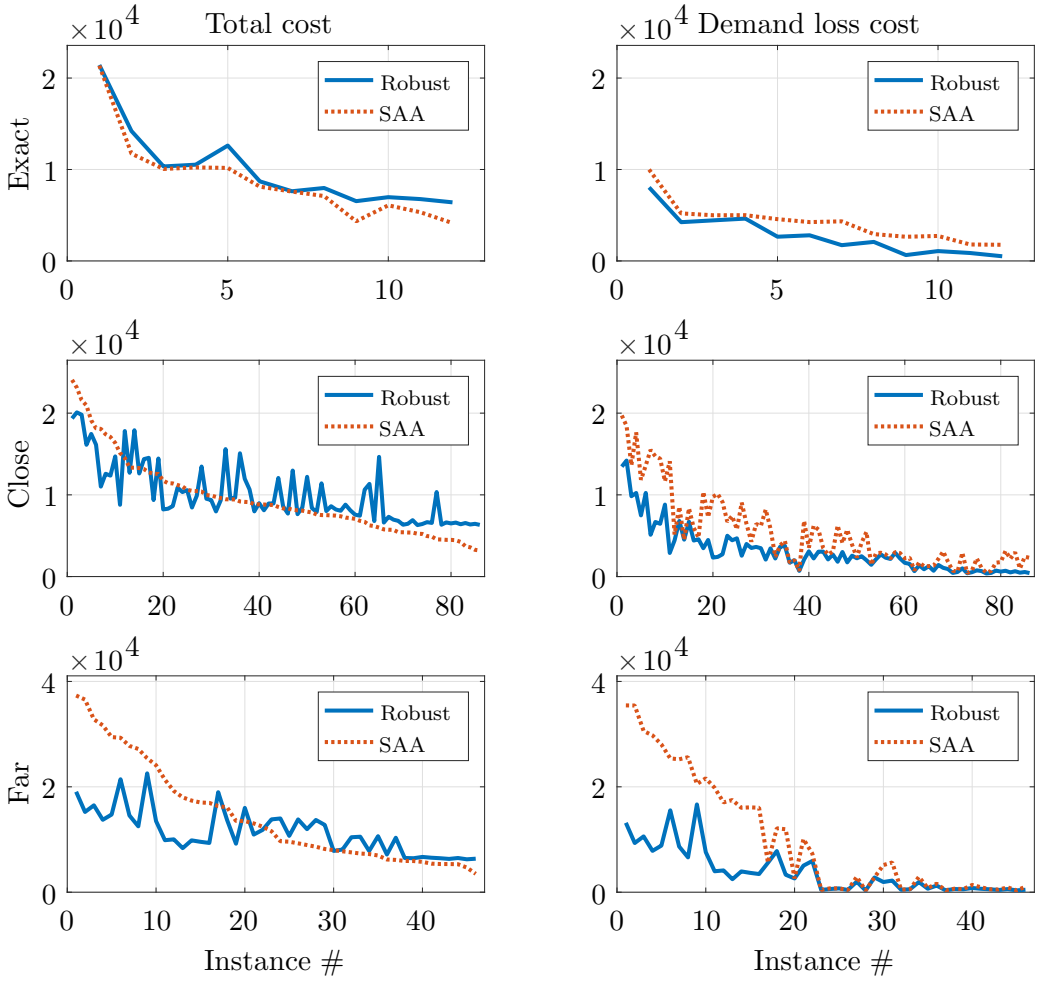

Figure 10 Objective values in 144 instances when evaluating the stochastic and robust solutions against actual probability distribution (sorted from highest to lowest SAA total costs).